Techno-economic evaluation of the electrochemical production of renewable ethylene oxide from fluctuating power sources and CO_2

Valerie Rodin [a,b,*], Hans Böhm [a], Johannes Lindorfer [a], Christian Paulik [b]

[a] *Energieinstitut an der Johannes Kepler Universität Linz, Altenberger Straße 69, 4040 Linz, Austria*
[b] *Institute for Chemical Technology of Organic Materials, Faculty of Engineering and Natural Sciences, Johannes Kepler University Linz, Altenberger Straße 69, 4040 Linz, Austria*

ARTICLE INFO

ABSTRACT

We present a techno-economic assessment of a novel ethylene oxide (EO) production process, which converts carbon dioxide (CO_2) and water electrocatalytically to ethylene (C_2H_4) and hydrogen peroxide (H_2O_2), which are further synthesized into EO. To ensure environmental sustainability, the primary focus was on available CO_2 from biogenic sources (biomethane and bioethanol plants) and renewable power sources (wind and photovoltaics) for decentralized applications. Accordingly, data on existing European CO_2 and renewable power sources were compiled for spatial analysis to develop technology roll-out and exploitation scenarios: 175 suitable locations were identified. Focusing on three locations, the production costs of EO and the product mix were calculated, considering various energy sources and plant configurations (as of 2030 and 2040). For a generic scenario, considering CO_2 to be available free of cost (existing biomethane upgrading) and electricity cost of 36€/MWh, the production cost of the product mix (EO, H_2O_2, methane, hydrogen) amount to 0.86 €/kg. This is at a similar order of magnitude as assessments on other Power-to-X value chains. Assuming that EO is the only utilizable product, the costs increase to 5.78 €/kg, which is significantly higher than for fossil alternatives. According to the sensitivity analysis, energy efficiency, electricity prices, and capital expenditure are the most relevant factors. Regarding the latter, an extended plant lifetime is a crucial factor.

1. Introduction

1.1. Chemical use of fossil resources

The annual global carbon demand amounts to 18,000 Mt, of which about 550 Mt are embedded in chemicals and derived materials. Regarding the latter, EU27 has a share of 110 Mt, about 90% are covered by fossil feedstock. [1] The use of fossil resources and CO_2 emissions of EU27 shall be reduced to net-zero by 2050 [2], in contrast, chemical markets are expected to grow significantly [1,3,4]. Thus, renewable carbon sources need to be tapped, to enable a sustainable transition of the chemicals and materials market, as there are no carbon-free alternatives available to great extent (e.g., for polymers or organic chemicals). Carbon sources available in the long-term are biogenic, recycled and atmospheric carbon.

Carbon Capture and Utilization (CCU) technologies are vital to close the anthropogenic carbon cycle, not only for climatic but also industrial reasons. Depending on the route, existing industrial infrastructure will be needed for downstream processing, which supports social, environmental and economic welfare. [5]

The need to replace fossil resources by renewable ones drives research into carbon dioxide (CO_2) conversion technologies and alternative carbon sources. Various projects aim to develop and implement CCU technologies for industrially relevant chemicals [6,7] via different approaches (such as biochemical, photocatalytic, thermal,

Nomenclature		J	Joule
		k€	thousand Euros
Chemical Formulas		kg	kilogram
C_2H_4	ethylene	kt	kilo tonne
CH_4	methane	km	kilometer
C_2H_4O	ethylene oxide	kWh	kilowatt hours
CO	carbon monoxide	m^3	cubic meter
CO_2	carbon dioxide	mA	milliampere
H_2	hydrogen	MJ	Megajoule
H_2O	water	MWh	Mega Watt hours
H_2O_2	hydrogen peroxide	Mt	Mega tonne
		t	tonne
Units		TW	terawatt
a	year	USD	United States Dollar
A	Ampere	V	Volt
cm^2	square centimeter	Wh	Watt hours
GWh	Gigawatt hours	€	Euro
h	hour		

chemo-enzymatic, electrochemical ones, cf. [8]). Thus, the potential for synergistic interlinking of the energy and chemical sectors grows, as electrification, fossil-resource phaseout and circular economy development progress. This means, electrochemical CCU routes are ideally i) suitable for the utilization of excess energy or off-peak power, and ii) come with scalability suitable for decentralized application as an adjunct to wind or PV parks and CO_2 sources.

1.2. Energy system transition

The phaseout of fossil resources does also change the energy landscape: wind power and photovoltaics (PV) are key technologies for renewable, sustainable energy systems. Apart from their immense potential to reduce greenhouse gas (GHG) emissions in power generation, they are characterized by a strongly fluctuating and intermittent power output [9–11]. According to the International Energy Agency (IEA), by 2050, wind and PV will produce up to 56% of electricity in the European Union (EU) [12], and wind power is expected to become the largest source of electricity shortly after 2030 in the EU. The increasing share of renewable energy sources (RES) has led the EU to address the challenges caused by large-scale integration. In the IEA 2050 net zero emission scenario, RES provide nearly 81% of global power capacity [12]. Fig. 1 shows the expected future RES capacity worldwide. Energy storage technologies can be used to harmonize the renewable power generation with the demand and stabilize the power grids [13–15]. The same
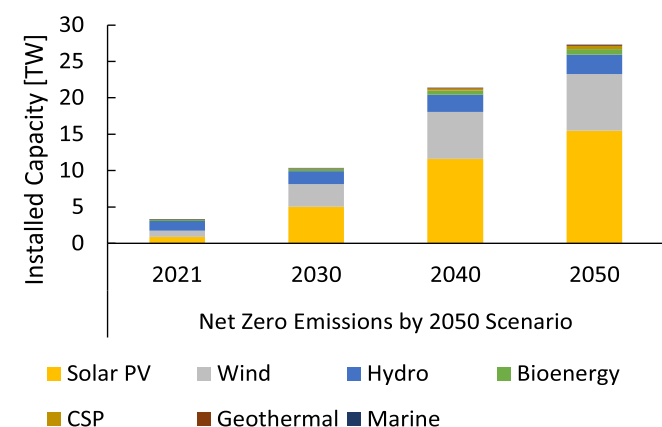
applies to Power-to-X (PtX) technologies, if their processes are designed and operated in a beneficial way [16,17].

1.3. Study focus

The subsequent study specifically focuses on the techno-economic assessment (TEA) of a novel PtX/CCU process for the production of ethylene oxide (EO; C_2H_4O, also known as oxirane or epoxyethane) on an industrial scale, taking into account already available RES potentials and biogenic CO_2 sources. The chemicals aimed at are ethylene (C_2H_4) and hydrogen peroxide (H_2O_2) produced from CO_2 and water in an electrochemical cell, followed by EO synthesis. With regard to ecological impact, the analyzed route (biogenic CO_2, wind or PV power) could lead to GHG emissions of up to − 0.15 to − 0.49 $kg_{CO2eq.}/kg_{EO}$ for a cradle-to-gate system boundary[1] according to Rodin et al. [18]. However, considering the European average grid mix, the GHG emissions would exceed the fossil benchmark [18]. Hence, RES were considered as the only viable option for the subsequent analysis.

1.4. Bulk chemical ethylene oxide

EO is one of the most versatile chemical intermediates, a bulk chemical that is mainly used in the production of ethylene glycols, surfactants, ethanolamines, and glycol ethers [19,20]. At the industrial scale, EO is mainly produced through the direct oxidation of ethylene with oxygen (O_2) and a recycled gas (EO, CO_2, and H_2O) in a catalytic reactor using Ag-based catalysts. Owing to thermodynamics, a large amount of heat is dissipated and CO_2 is generated as an unwanted byproduct [21].

Global markets for ethylene and its derivatives, ethylene oxide (EO) and ethylene glycol, are driven by growing demand from PET bottle manufacturers, the textile industry, and the automotive industry (as antifreeze), among others. According to a market report published by Transparency Market Research [22], the global EO market is dominated by the Asia/Pacific, North America, and Western Europe. The average market prices for ethylene, EO, and mono ethylene glycol are compiled in Fig. 2. The global market volume of EO is expected to grow to > 36 million tons in 2030 [20], with a market value of about 72 billion USD [23].

Fig. 1. Prognosis of future installed RES power. Based on IEA (2022) World Energy Outlook 2022. [12].
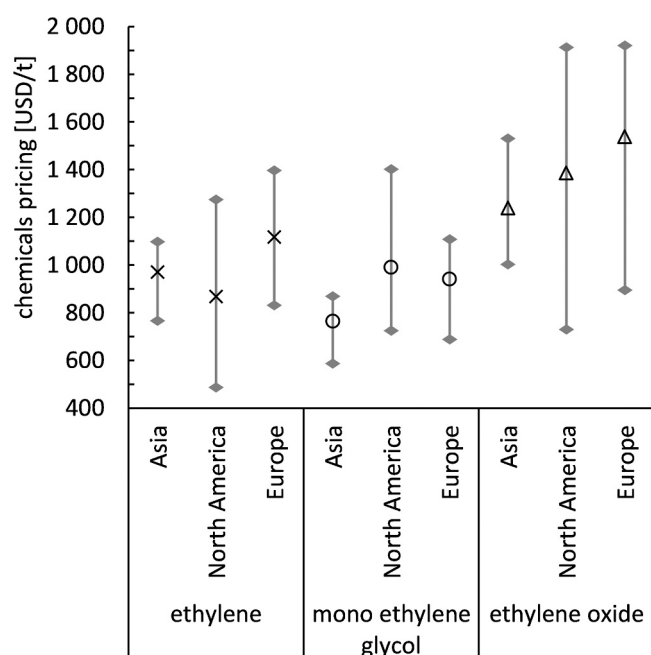
---

[1] Based on mass allocation, no credits

Fig. 2. Market prices for ethylene, ethylene oxide & ethylene glycol from 2021 to 2022. Based on data from [24–26].

1.5. Alternative production routes for EO

Alternative production options for C_2H_4 [27–32] and EO [21,33,34] are of increasing research interest. Electrochemical routes are at the lowest level of maturity [8,35,36]. If successfully developed and implemented, they promise radical innovations in the chemical production sector. In recent years, the focus of EO research (e.g., Mobley et al. [37]) has shifted towards replacing O_2 with CO_2.

1.6. Novelty of the studied process

One novelty of the CCU process is that instead one-carbon (C1) compounds (e.g., methane, methanol, carbon monoxide) are in focus but the more complex formation [38] of ethylene, a two-carbon (C2) compound (see also ethanol [39], acetate [40], dimethyl ether [41,42] i.a.). As ethylene is a base chemical, research focus shifted towards the development of suitable processes in recent years [38,43,44].

Also, in contrast to many other PtX paths, the CO_2 is directly converted through electrocatalytic reduction. That is, without the intermediate step of water electrolysis for hydrogen (H_2) production and downstream CO_2 hydrogenation. Compared to these widely studied approaches, though, direct CO_2 reduction is currently less advanced [45].

Another novelty is that both half-cell intermediaries are further synthesized into EO: in theory, the utilization of all anodic and cathodic electrocatalytic products and the reduced number of conversion steps allows to increase the overall energy and resource efficiency compared to other PtX/CCU routes.

2. Methods

2.1. Study context

This article presents parts of a socio-economic impact assessment, which was carried out within the EU Horizon 2020 project CO_2EXIDE [46,47]. It contains a combined spatial analysis and TEA. The analysis is complementary to the life cycle assessment for the process and CO_2 potential analysis performed in previous studies [18,48]. Fig. 3 provides an overview of the analysis steps: i) a resource potential study for Europe

was conducted, ii) followed by the TEA for a generic case and three exemplary locations.

2.2. Potential and spatial analyses

The European market potential for a theoretical technology readiness level (TRL) of 7–9 was assessed. This included i) review of total CO_2 availability in Europe based on [48], iii) spatial analysis of European biogenic CO_2 point sources and RES (software: QGIS [49]), and iv) analysis of favorable conditions (short distance to resources).

For the spatially resolved CO_2 and RES, datasets on bioethanol [50], biomethane [51,52], PV plants (>1 MW) [53], and onshore wind farms (1–5 MW and >5 MW) [53] were used; for more information, refer to the Appendices A and B. The data were classified based on the type (CO_2 from bioethanol or biogas; wind or PV power) and amount of CO_2 (t/a), or power capacity (MW).

For the localization of large PV and wind farms across Europe, basic information as of 2019 was collected using the Power Plant Tracker [53], wind farm database [54] and specific company websites (power plant and grid operators and manufacturers).

Grid-bound or direct line, short-distance transmission of renewable electricity was favored over CO_2 transport, and RES sources outnumbered CO_2 point sources; thus, a matching of resources was performed: PV and wind farms were selected based on their location within a 5 km radius around each CO_2 source. For some CO_2 sources, more than one RES within the 5 km range was available. Next, the amount of locally produced renewable energy was compared with the amount of available CO_2 for each match. Finally, three locations in Austria, Germany, and the United Kingdom (UK) were chosen as case studies.

2.3. Techno-economic indicators

How the TEA was executed in detail is outlined in Section 3. Below, the evaluated indicators are explained: Net Present Value (*NPV*), Payback Time (*PBT*) and Levelized Cost of Production (*LCoP*).

2.3.1. Net present value
The *NPV*, as defined in Eq. (1), is a common measure used in dynamic investment evaluation. It is defined as the sum of all current and future cash flows (R_t) of an investment discounted to the present. Linear depreciation was assumed, so capital expenditure (CAPEX) was distributed evenly over the observation period.

$$NPV(i, N) = \sum_{t=0}^{N} \frac{R_t}{(1+i)^t} \tag{1}$$

where i = interest rate N = total number of periods t = time of cash flow R_t = cash flow at time t.

For R_t, expenditures are represented as negative values and include CAPEX and fixed operational expenditures (OPEX), as well as the annual costs of feedstock materials and energy inputs. Potential revenues from (by)product sales are represented as positive values. Consequently, $NPV > 0$ indicates a positive value added, while $NPV < 0$ indicates a negative value added, and is therefore an indicator against an investment.

2.3.2. Payback time
The payback time (*PBT*) as defined by Eq. (2) indicates the minimum operation time, which is essential for the plant to become profitable.

$$PBT = \frac{I}{\sum c + \sum r} \tag{2}$$

where.

I = total investment cost (CAPEX).

$\sum c$ = total annual costs.

Fig. 3. Procedure of GIS-based potential analysis and subsequent TEA for Europe.

$\sum r$ = total annual revenue.

The shorter the *PBT*, the more profitable is the operation of the plant and the earlier a net profit is generated, whereas a *PBT* < 0 indicates non-profitable operation of the plant.

2.3.3. Levelized cost of production

To estimate potential production costs, the levelized cost of production (*LCoP*) was calculated as an appropriate specific indicator and compared to similar evaluations performed in other PtX assessments [55]. The approach is similar to the commonly used levelized cost of electricity (*LCoE*) method [56]. We considered a full year of operation in

which the total annual cost is calculated using the annuity method [57].

$$LCoP = \frac{-A + \sum_i C_{var,i}}{M_{out}} \tag{3}$$

where.

A = annuity of the fixed total annual payments, such as capital- and operation-related costs.

M_{out} = total annual product mass-related output.

C_{var} represents variable cost and revenues that depend upon the corresponding material and energy streams, and are, thus, related to the annual time of operation and potential variable load conditions, such as

part-load efficiencies. These include demand-related cost for resources such as electricity, CO_2, and H_2O, as well as potential byproduct sales. For the calculation procedure of *A* and further factors, refer to Appendix H.

To address potential future cost reductions through technological learning, corresponding effects were evaluated for all the above indicators by considering the learning rates for individual components and properties specific to the investigated technology. With this approach, changes in the overall cost structure can also be analyzed, and the potential leverage for cost reduction may be discovered in the early stages of technology maturity. A detailed description of the model and its application for power-to-gas technologies were described elsewhere [55, 58].

3. Techno-economic assessment

3.1. Scope of the study

The TEA aimed to identify the economic performance of the electrochemical process chain in a technically feasible industrial implementation. With a TRL of 3–4, an according process evaluation and optimization based on actual implementation in the relevant industrial environment are not possible. Thus, the development of the technology towards industrial scale-up must be anticipated based on the available data, expert elicitation, consideration of individual component maturities, and relevant literature. Additionally, the economic impacts of technology scale-up, both in terms of the numbers and individual scale, potential byproducts and regulatory measures - compared with fossil competitive products - must be considered in an appropriate manner. The period under consideration was 20 years, with an assumed start of operation in 2030 or 2040. Process data input was based on laboratory measurements and modelling [18,47,59–61] as well as state-of-the-art literature data.

3.2. Fossil product benchmarks

Fossil-based EO and their precursors were considered as benchmark products. The production of these bulk chemicals is well-established. Currently, state-of-the-art EO production involves direct oxidation, in which C_2H_4, O_2, and a recycled gas are mixed in a catalytic reactor [21, 62], resulting in the formation of EO, CO_2, and H_2O [62]. The most common process for producing C_2H_4 is steam cracking of gas, other hydrocarbons, or naphtha, that is, a fraction of crude oil distillation [63].

According to Plastics Europe [64], in 2012, approximately 9% of production costs accounted for energy consumption, and in some extreme cases, energy input was responsible for approximately 75% of production costs, with a reduction in the average specific energy requirement of 30% compared to the value in 1990. In October 2019, the 2050 roadmap [63] of the German chemical industry was published, which reviewed the future development of steam cracking products (high-value chemicals, HVC), such as C_2H_4. Based on this study, the following benchmarks for fossil HVC were derived:

Considering an average energy input of 4.582 MWh/t_{HVC} [2] and CO_2 emissions of 0.87 t_{CO2}/t_{HVC} from conventional crackers and 2.22 t_{CO2}/t_{HVC} from electrical crackers in 2020, the total specific production cost is approximately 820 €/t_{HVC} for conventional crackers and 930 €/t_{HVC} for electrical crackers. Consequently, for conventional crackers, the energy cost accounts for about 235 €/t_{HVC} [3] (28.7%), and the CO_2 emission cost amounts to 21.75 €/t_{HVC} (2.65%). Meanwhile, for electrical crackers,

the energy cost accounts for about 183.3 €/t_{HVC} [4] (19.7%), and the CO_2 emission cost amounts to 55.5 €/t_{HVC} (5.97%).[5] However, it is noteworthy that the higher CO_2 emissions from electrical crackers (new technology) compared with conventional crackers originate solely from the German electricity mix in 2020 and will be reduced to zero in the long-term scenario by 2050 anticipating a renewable electricity mix.

While these figures serve as general benchmarks, the target product of the investigated process was EO. Steam-cracked C_2H_4 oxidized with O_2 or air to EO using silver catalysts served as a conventional reference technology. The benchmark process is described in the literature [21, 65], with large-scale industrial-scale simulations and TEA/LCA.

3.3. Reference unit

All specific cost assessments were related to a reference unit of 1 kg EO. Additionally, 1 kg of the product mix was used as a reference to demonstrate the impact of resource and energy efficiency.

3.4. Boundary conditions

A cradle-to-gate scenario was assumed, from the CO_2, water, and electricity supply to the EO as the final product. Cost factors were attributed to reflect the source of material and energy inputs. As shown in Fig. 4, the intermediates C_2H_4 and H_2O_2 are produced from water and CO_2 in an electrocatalytic unit (ERU). In the next steps, the intermediates are enriched (EEU) and reacted to synthesize the final product (EOU). In terms of realization, these concepts have been proven at the laboratory scale within the project.[6] The byproducts H_2 and CH_4 can be valorized as marketable products or utilized on-site; however, the latter was not examined. Surplus H_2O_2 can also be marketed.

3.4.1. Electrical energy
Electrical energy was supplied either by purchasing electricity from the grid or from a local RES plant such as wind or PV. For the latter, the energy cost was calculated based on the energy availability and levelized cost of electricity (LCoE) to represent the assessed source.

3.4.2. CO2
To ensure climate-neutral CCU products, the use of biogenic CO_2 from existing industrial point sources was targeted (cf. Rodin et al. [48]), being defined as carbon-neutral [68]. The major sources include the combustion of biomass, CO_2 from biogas upgrading, and industrial fermentation processes such as bioethanol production [48]. Atmospheric CO_2 (DAC) and CO_2 from combustion were excluded, as they require high technical capture and purification efforts [48].

Alternative scenarios out of scope were the utilization of CO_2 from other industrial point sources and direct air capture (DAC) to meet the industrial carbon demand [69], and to utilize unavoidable CO_2 [5,70] in a closed carbon cycle.[7]

The CO_2 feedstock was assumed to be supplied by a nearby biogenic stationary industrial process via a short, direct line or process integration. CO_2 separation technology and process were not included in the TEA in detail, while a specific CO_2 price was considered to cover

---

[2] Conversion from 16.5 GJ/t_{HVC} derived from [63].

[3] Assumption: energy demand covered by oil/ gas at an energy price of 98 $/barrel. Assuming 1.20 $ = 1.00 €, 158.9873 l/barrel, and 10 kWh$_{LHV}$/l, an average energy price of 5.137 ct/kWh$_{LHV}$ is calculated [63].

[4] Calculated based on data from [63].

[5] Assuming 4 ct/kWh$_{el}$ (neglecting taxes, levies, and CO_2 emission-prices) and 25 €/t_{CO2} [63].

[6] Note that in the experimental setup for safety reasons, the EO was further reacted in excess H_2O (hydrolysis) to yield ethylene glycol [66,67].

[7] As the focus was on long-term, fully renewable alternatives, another potential scenario was out of scope as well: a CCU process integration into existing steam crackers (fossil EO route) for on-site CO_2-emission conversion [18,71]. While direct CO_2 emissions would be reduced [72], the EO output would increase without reducing the absolute demand for fossil resources, considering growing EO markets.
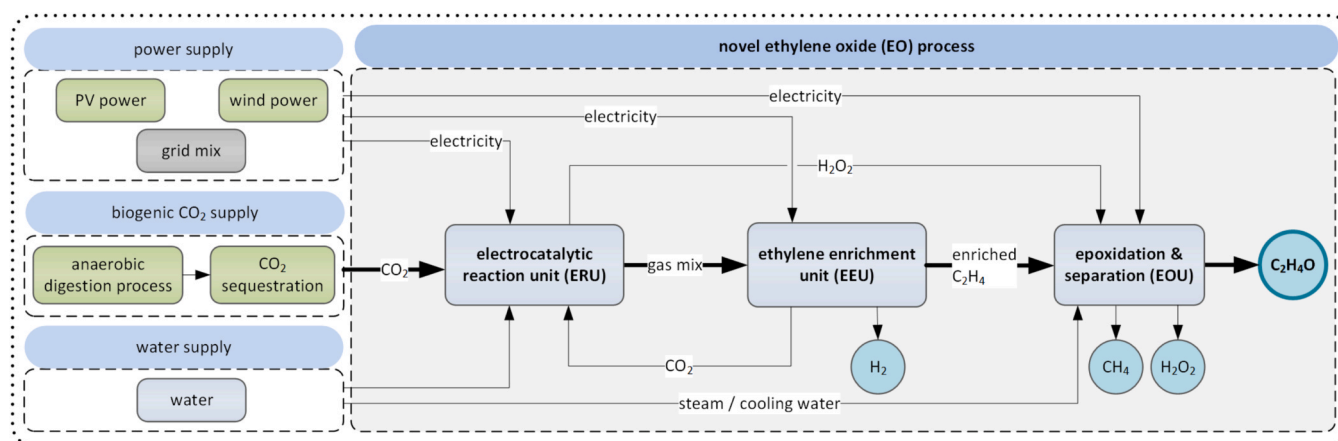
Fig. 4. System boundaries and scheme of the assessed process.

potential capture costs. See also Sections 3.6.4.2 and 4.3.

3.4.3. Water

Water was assumed to be supplied via the local water network, and the costs were taken from [73].

3.5. Application scenarios

3.5.1. Generic case

The generic case was built upon a given hourly CO_2 input (without recycled CO_2) of about 394 kg/h, corresponding to the average CO_2 available at the biomethane upgrading plant Bruck/Leitha[8] (see Section 3.5.2.1). The single-pass conversion rate of CO_2 of the electrocatalysis was approximately 19% in the 2030 scenario, with surplus CO_2 being recycled. The total CO_2 input was approximately 2031 kg/h. For the 2040 scenario, a single-pass CO_2 conversion rate of 50% was assumed. The Faraday efficiencies (FE) and selectivities of C_2H_4 and H_2O_2 were kept constant at 48% throughout the scenarios.

The power demand for the electrocatalysis was estimated with 11.67 MW_{el}. For 2040, 5.25 MW_{el} was assumed due to the increased energy efficiency. Refer to Section 3.6 regarding the detailed input data and calculation procedures. For electricity input, the average EXAA (Energy Exchange Austria) green spot market price in 2019 was assumed.

For EO synthesis, the ethylene epoxidation unit by [21] was used as a reference, considering the specific electrical energy, steam, and cooling water demands per kilogram of EO as well as their conversion efficiencies. Assumptions regarding the ethylene oxide synthesis unit's (EOU) parameters were assumed to be constant across all scenarios; as such, for the 2030 scenario, the efficiency has been predicted to be rather high [21].

3.5.2. Case studies based on spatial analysis – boundary conditions

In addition to the generic case, three case studies were derived from spatial analysis. They differed in terms of available CO_2, RES, and local conditions: the focus was on varying the availability of basic resources. Also, EO is produced and consumed globally but is a hazardous chemical to transport [74–76]. Regional production would therefore be suitable regarding reduced transport needs to customers. As shown in Fig. 5, 175 locations offering biogenic CO_2 and RES within close proximity were identified.

Three European locations were selected for detailed case studies. The distances between the CO_2 sources and RES plants were analyzed in

more detail and adjusted if necessary. Finally, proximity to pipelines or large industrial facilities played a crucial role in the final selection of sites. The three selected sites are described below.

3.5.3. Bruck/Leitha, Austria - the benchmark plant

The Austrian location provides CO_2 from a biogas plant with bio-methane upgrading, Table (D.1) summarizes the basic site data. The production capacity is 500 m^3/h of biomethane [51]. This results in a theoretical feedstock of 5280 t_{CO2}/a, assuming a CO_2 content of 40%vol. and 8000 full-load hours (FLH) per year. Based on on-site investigation, an actual potential of approximately 3370 t_{CO2}/a was used for case-specific calculations.

Two wind farms with close proximity (approximately 7 km) were identified for the renewable power supply, see Fig. (D.1). The total installed capacity is 30 MW. Based on historical weather data, an annual energy production of approximately 96.3 GWh/a was calculated with renewables.ninja.com [84], see Fig. (D.2). The annual energy generation data available from the plant operator [85,86] sum up to approximately 66 GWh/a, that is, 30% lower than the modelled data. This discrepancy may be explained by the planned and unplanned shutdowns and un-considered inefficiencies in the simulations. The lower values were considered in the TEA.

Furthermore, large chemical industry (Schwechat refinery [87]) lies in a relatively close range to Bruck/Leitha (ca. 27 km), including the starting point of an intra-national C_2H_4 pipeline (see Appendix D.1).

3.5.4. Zerbst, Germany

In the second case, Energiepark Zerbst, an energy model park in northeastern Germany, was identified as a suitable option. See Table (D.2) for basic location data and Fig. (D.3). The site offers PV and wind power capacities, and a biomethane plant. The latter has an annual biomethane production capacity of 770 m^3/h [51]. Considering the previously described average conditions, the theoretical CO_2 potential is 8131 t_{CO2}/a.

The installed PV capacity at Zerbst is 30 MW_{peak}. Theoretical PV generation was simulated using the online simulation tool PVGIS [88], leading to an annual electricity generation of approximately 52 GWh/a. The wind power generation was calculated to be approx. 57.7 GWh/a based on 46 MW installed capacity [84], see Fig. (D.4). Again, differences from the actual generation are likely. As no literature data was available, the simulated generation profiles were used.

Leuna Chemical Park [89] is located 75 km south of Zerbst, i.e., the possibility of selling the products to nearby industries was considered quite likely.

3.5.5. Isle of Wight, UK

The third location is Isle/Wight, located close to the southern coast of

---

[8] Note: This plant served as a reference and CO_2 source for the underlying research project.
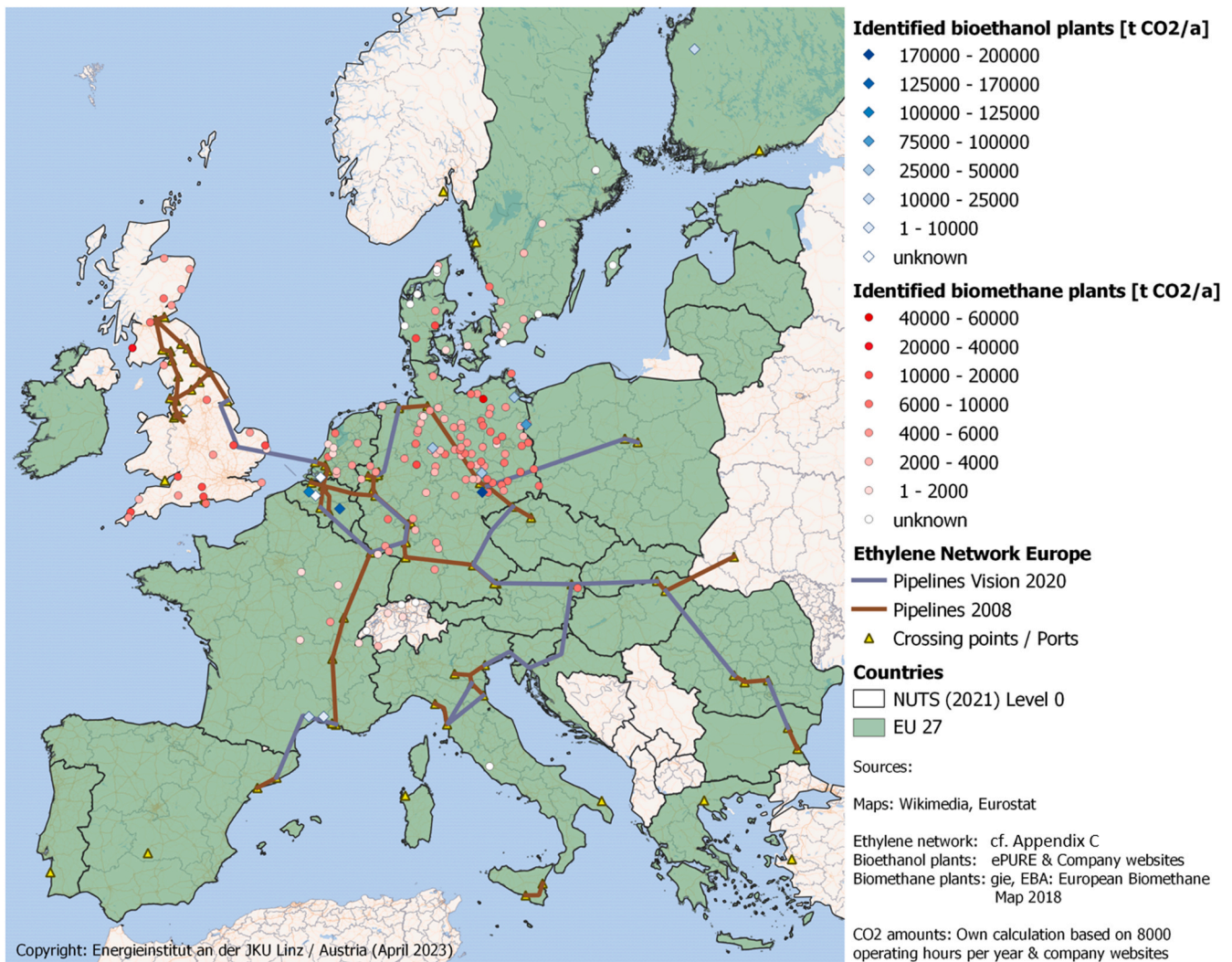
Fig. 5. Biomethane upgrading (162) and bioethanol (13) plants with PV plants/wind farms within a 5 km range available. Also, existing ethylene pipelines are displayed. Based on [50,51,77–83] and specific company websites.

Table 1
Overview of the simulated energy production for the combined RES considered in the three cases.

	Unit	Bruck/Leitha	Zerbst	Isle/Wight
Cumulated installed RES capacity	MW	30	76	28.7
Total energy generated	MWh	96344	Total: 109659 PV: 52006 Wind: 57658	27138
Average energy generated	kWh/h	10998	12518	3089
Share of hours with no production	%	0	0	53
Share of hours with production < 100 kWh	%	0	0	54
Share of hours with production < 10% of average	%	9	5	56
Share of hours with production > = average	%	45	38	28

the UK. Table (D.3) summarizes the basic location data of an existing biomethane, see also Fig. (D.5). The theoretical CO_2 potential was approximately 6300 t_{CO2}/a at average conditions. Relevant literature on upgrading technology states a slightly higher value of 6900 t_{CO2}/a, likely due to a higher CO_2 content of 45%vol. for the raw biogas [90].

Several PV plants are in close proximity, which could serve as RES. For the TEA, four PV plants were considered within a range of ca. 5.5 km around the biogas plant. The peak capacities ranged from 4.8 to 10.6 W, adding up to 28.7 MW. Owing to a lack of production data, the annual energy generation was simulated [88]. With approximately 27 GWh/a, the power supply potential was significantly lower than that for the

other cases (see Table 1 and Fig. (D.6)).

A seaport at about 10 km distance was identified to provide a potential additional benefit for future electrochemical process implementation. In a distance of 20 km from the mainland, the UK's largest conventional refinery is located in Fawley, near Southampton, see Fig. (D.5).

3.5.6. RES availability and quality

The characteristic of wind and solar energy production to be volatile is relevant for the operation of electrochemical processes with direct RES supply. The type of energy generation significantly affects the
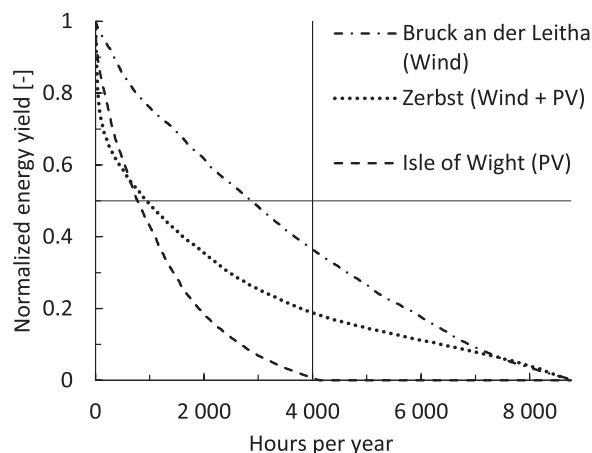
Fig. 6. RES load duration curves at the three cases. Modelled with [84].

Table 2
Overview of process streams.

Streams	Value (2030)	Value (2040)	Unit
Feedstock			
Carbon dioxide (CO_2)		3.0	kg/kg$_{EO}$
CO_2 recycle stream	12.9	3.03	kg/kg$_{EO}$
Water (H_2O)		10.8	kg/kg$_{EO}$
Intermediates			
Hydrogen peroxide (H_2O_2)		6.16	kg/kg$_{EO}$
Ethylene (C_2H_4)		0.85	kg/kg$_{EO}$
Of which further utilized		0.65	kg/kg$_{EO}$
Products			
Ethylene oxide (C_2H_4O)		1	kg/kg$_{EO}$
Byproducts			
Hydrogen (H_2)		0.15	kg/kg$_{EO}$
Methane (CH_4)		0.13	kg/kg$_{EO}$
Hydrogen peroxide (H_2O_2)		5.39	kg/kg$_{EO}$
Losses/recycled intermediates			
Ethylene (C_2H_4)		0.20	kg/kg$_{EO}$
Hydrogen (H_2)		0.17	kg/kg$_{EO}$
Methane (CH_4)		0.002	kg/kg$_{EO}$

a with > 20% capacity.

Thus, the direct utilization of electricity production from fluctuating RES requires appropriate flexibility of the downstream PtX process. This might be mitigated by integrating intermediate electricity-storage capacities, which flatten the energy-supply pattern. Alternatively, PtX processes can be operated in a grid-supportive manner through load balancing or peak-shaving [91]. E.g., a defined base generation can be delivered to the grid, while the volatile generation peaks supply the electrochemical plant. Owing to the uncertain operational characteristics of the analyzed technology regarding flexibility, no appropriate supply profile was evaluated. Thus, the potential economic benefits of grid-supportive operation were excluded in this study.

3.6. TEA input data inventory

The following sections explain the design and modeling of the process. Table 2 summarizes the major process streams. Slight modifications compared to [18] were made to facilitate modelling.

3.6.1. Electrocatalytic reaction specifications

As previously described [18], the ERU comprises two half-cells, with a cathodic CO_2RR to C_2H_4 and an anodic WOR to H_2O_2. The cathode of the demonstrator comprised a copper sputter deposited on a Freudenberg gas diffusion layer, whereas a boron-doped diamond/niobium electrode served as anode. Each chamber was supplied with an electrolyte solution at different concentrations and separated by a membrane, of which various were tested [47]. Finally, a commercially available Nafion membrane was used. The cell design is comparable to that of commercial hydrogen proton exchange membrane (PEM) cells. Ideally, half-cell reactions according to Eq. 4 and Eq. 5 take place, leading to Eq. 6 (Table 3).

Accordingly, the theoretical cell potential amounts to (1.76 – 0.064) V = 1.696 V, considering thermodynamic effects of operating conditions, it amounts to 1.68 V [93]. This value was considered the minimum viable cell potential; thus, equaling 100% voltage efficiency, an auxiliary parameter introduced for the TEA.

In reality, higher voltages are needed to prevent competitive reactions, such as O_2 evolution through H_2O splitting at the anode or production of hydrocarbons other than C_2H_4 at the cathode. Furthermore, the selected components affect the overall cell potential and reaction selectivities. Also, the current density is critical, determining the possible amount of desired products and selectivity [73,92,94]. The demonstration unit was equal to the one described in [18]; current densities of 150–200 mA/cm^2 with an active cell area of 300 cm^2 and a cell voltage ≤ 10 V were applied.

For the large-scale TEA scenarios, optimized conditions were assumed (Table 6), and the electrical power input P [W] was calculated from the theoretical voltage and current as U [V] × I [A]. The latter, that is, the electrons required to convert CO_2 and H_2O, was calculated based on the given FE_{C2H4} and FH_{H2O2} (Eq. 7), according to Jouny et al. [73]. In contrast to [73], this method was not only followed for the cathodic main product C_2H_4 but also for the anodic product H_2O_2. The active cell area was calculated from I [A] and given current densities. As the ERU half-cells were coupled, the same electrical specifications were assumed for both, whereas the cathodic chamber served to specify the main parameters and the anodic production was adjusted accordingly.

temporal availability of electricity for the process (see Table 1). Comparing the Austrian and British cases with similar RES capacities, the first is supplied with wind energy most of the year, whereas the latter relies on PV, and no energy is generated for approximately six months (53%) owing to strong daily and seasonal fluctuations. The total energy generation was 3.5 times higher in the Austrian scenario. Although the hybrid supply in the German case prevents hours of no electricity production, annual total and average generation are only about 12% higher than in the Austrian case despite 2.5 times higher capacity.

The normalized RES load duration curves of each case in Fig. 6 underline the results. The wind power generation at Bruck/Leitha exceeded 35% of the nominal capacity by nearly 4000 h/a. In comparison, the Isle/Wight PV plants exhaust their capacity for only a few hours per year: 50% capacity is available for < 1000 h/a, and energy is generated only throughout ca. 4000 h/a. The hybrid generation at Zerbst results in a mixed load duration curve, with even lower full capacity hours than the Isle/Wight and about 1000 h/a at half capacity, but approx. 4000 h/

Table 3
Half-cell reactions resulting in C_2H_4 and H_2O_2 formation based on CO_2 and H_2O.

Reaction type	Reaction equation	Reaction potential	Source	Eq. #
CO_2 reduction reaction (CO_2RR)	$2CO_{2(g)} + 12 H^+ + 12e^- \rightarrow C_2H_{4(g)} + 4 H_2O_{(l)}$	Potential (V vs. SHE) = 0.064 V	[73]	Eq. 4
Water oxidation reaction (WOR)	$2 H_2O_{(l)} \rightarrow H_2O_{2(l)} + 2 H^+ + 2e^-$	Potential (V vs. RHE) = 1.760 V	[92]	Eq. 5
Redox reaction	$2CO_{2(g)} + 12 H^+ + 12e^- + 12 H_2O_{(l)} \rightarrow C_2H_{4(g)} + 4 H_2O_{(l)} + 6 H_2O_{2(l)} + 12 H^+ + 12e^-$			Eq. 6
	$2CO_{2(g)} + 12 H_2O_{(l)} \rightarrow C_2H_{4(g)} + 4 H_2O_{(l)} + 6 H_2O_{2(l)}$			

Source: Reproduced with permission from Rodin et al. [18].

Table 4

Electrochemical reactor unit's characteristics, in accordance with [18].

Parameter	Unit	2030	2040	Source
Electric characteristics				
Current density	A/cm^2	0.50	0.50	[18]
Voltage efficiency	%	36	80	[18]
Cell voltage theoretical	V	1.68	1.68	[93]
Cell voltage applied	V	4.67	2.10	calculated
Power demand	MW	11.67	5.25	calculated
Efficiencies				
Product selectivity cathode (FE$_{C2H4}$)	%	48	48	[18]
Conversion efficiency cathode	%	19	50	[18]
Product selectivity anode (FE$_{H2O2}$)	%	48	48	[18]
Conversion efficiency anode	%	0.10	10	[18]

Table 5

EEU and epoxidation reactor characteristics.

Parameter	Unit	Value	Note/Source
EEU			
Power demand EEU	kWh/kg$_{C2H4recov.}$	3.37	based on[18,95]
Power demand H$_2$/CO$_2$ separator	kWh/kg$_{H2+CO2recov.}$	0.13	
Ethylene recovery rate	%	76.77	
Epoxidation reactor			
Power demand	kWh/kg$_{EO}$	0.339	based on[21,65]
Steam demand	kg/kg$_{EO}$	0.740	
Cooling water demand	m^3 /kg$_{EO}$	0.463	
Selectivity to C$_2$H$_4$O	%	99	
Conversion efficiency	%	90	
Mass ratio H$_2$O$_2$/C$_2$H$_4$O	-	0.7721	stoichiometric calculation
Mass ratio C$_2$H$_4$/C$_2$H$_4$O	-	0.6368	

$$Q = \frac{z*n*F}{FE} \tag{7}$$

where.

Q = charge passed, that is, current I [A].

z = number of required electrons to produce a given product [-].

n = number of moles of a given product [mol].

F = Faraday constant [Coulomb/mol].

FE = selectivity of a given product [%].

From the mass flow and the molar mass of C$_2$H$_4$ (28 g/mol), n was calculated. The cathodic byproducts were accounted for with product ratios (kg$_x$/kg$_{C2H4}$) based on experimental results and projections performed during the project [95]. The byproducts added to the total CO$_2$ and water inputs as well as product revenues.

3.6.1.1. Electrocatalytic reaction selectivity. To determine realistic selectivities for C$_2$H$_4$ and H$_2$O$_2$, a literature review was conducted [18]. According to [18], for C$_2$H$_4$ and H$_2$O$_2$, selectivities of up to 70% and even more have been reported. Thus, in accordance with the experimental work conducted [47], 48% selectivity was assumed for both C$_2$H$_4$ and H$_2$O$_2$ for large-scale application scenarios (2030 and 2040). As the chemical reactions of multi-output processes are interdependent and the selectivities add up to 100% per half-cell, increasing FE$_{C2H4}$ must decrease the selectivity of the byproducts, but not necessarily linearly. Thus, in the absence of projections for selectivities in 2040, they were assumed to be constant to avoid estimation errors.

3.6.1.2. CO$_2$ conversion efficiency. In addition to selectivity, single-pass conversion efficiency is important in terms of the overall energy efficiency. This is particularly true for CO$_2$ conversion, where unreacted CO$_2$ must be separated from gaseous C$_2$H$_4$ and returned to the cathode. For the anodic reaction, single-pass conversion was considered less critical because the reactions occur in an aqueous solution: unreacted water is recycled in the electrolyte circuit. However, high concentrations are desired to decrease the energy demand for product separation and losses.

To increase the CO$_2$ utilization rate, CO$_2$ recycling was achieved with an ethylene enrichment unit (EEU) and process integration into a biogas upgrading plant. According to literature, a 10–50% CO$_2$ to C$_2$H$_4$ conversion rate may be realized in the future, depending on the electrocatalytic CCU route [73,96]. Table 4 shows the conversion efficiencies chosen based on experimental findings and literature [18]. Simultaneously, additional byproducts may be formed, which can aggregate in considerable amounts and be of value; thus, some of these were considered in the TEA.

3.6.2. Ethylene enrichment unit

Several technologies are available for the enrichment of the (intermediate) product C$_2$H$_4$, such as pressure swing adsorption (PSA), physical absorption, and membrane separation. The EEU was designed as a two-stage membrane separation unit using electrical compressors. Table 5 shows the specific energy demand for C$_2$H$_4$ separation alone and subsequent CO$_2$ recycling and H$_2$ separation. Because the CO$_2$ conversion efficiency (Table 4) is rather low in the 2030 scenario, approx. 6 kWh$_{total}$/kg$_{C2H4recov.}$ was calculated as the total specific EEU energy demand, including the energy required for the separation of H$_2$ and unreacted CO$_2$ [18]. For the 2040 scenario, it was decreased to about 4 kWh$_{total}$/kg$_{C2H4recov.}$, as the amount of recycled CO$_2$ will be lower due to the higher single-pass conversion efficiency [18]. Moreover, the EEU separates unreacted CO$_2$ and other byproducts from C$_2$H$_4$. The separated streams can then be recycled on-site (particularly CO$_2$), fed into the gas grid (CH$_4$ and H$_2$ to some extent), or sold directly (H$_2$). Note that the byproduct CH$_4$ was assumed to be separated in the EOU process.

3.6.3. Ethylene oxide synthesis

The synthesis of EO (C$_2$H$_4$O) from H$_2$O$_2$ and C$_2$H$_4$ was modelled in accordance with the assumptions made in [18]. According to future large-scale scenarios by Ghanta et al. [21,65], a > 90% single-pass conversion rate for C$_2$H$_4$ (unreacted C$_2$H$_4$ is recycled) and > 99% selectivity for EO are achievable (Table 5). The EO-specific steam and electricity demands were calculated based on [21,65]. Ghanta et al. [21]

Table 6
Economic calculation parameters.

Parameter	Unit	2030	2040	Source
General				
Interest rate	%	3	3	assumption
Observation period	years	20	20	[97], based on overall plant lifetime
Deprecation period (NPV calculation)	years	20	20	[97], based on overall plant lifetime
OPEX				
OPEX Maintenance	% of CAPEX	7	7	[98]
OPEX Insurance	% of CAPEX	1	1	[98]
Plant overhead	% of OPEX	50	50	[98]
Electricity costs				
Grid supply	€/MWh	35.6	35.6	[99–101], no projections for future grid electricity costs made
PV direct supply	€/MWh	55 *	30	[102], *Sustainable Development Scenario* * 2019 Europe values used from the reference
Wind direct supply	€/MWh	55 *	45	[102], *Sustainable Development Scenario* * 2019 Europe values used from the reference
Feedstock costs				
CO_2	€/t	0	0	[48], lower range value for biogas upgrading
Water	€/m³	1.26	1.26	based on [73]
Cooling water	€/m³	0.019	0.019	based on [21]
Steam	€/kg	0.016	0.016	based on [21]
Product Revenues				
Ethylene	€/kg	0.75	1.50	based on [103]
Hydrogen Peroxide	€/kg	0.50	0.50	based on [104]
Ethylene Oxide	€/kg	1.50	3.00	based on [24] / assumption
Methane	€/kWh	0.05	0.15	based on [105] and [55] for renewable methane production in 2040
Hydrogen	€/kWh	0.10	0.08	based on [55] for renewable hydrogen production
Additional				
CO_2 ETS price	€/t	50	100	for 2030 the average 2021 price was assumed; assumption for 2040

reported methanol as an additional solvent to water, which was recovered after EO separation with small amounts of catalyst promoter. These additives were not considered in this study because of their recyclability and small amounts respectively.

3.6.4. Economic parameters and assumptions

Table 6 summarizes the economic parameters. The calculation of the individual cost factors is described below. All cost data from the literature were normalized to 2021 values to encounter currency conversion rates and inflation, based on Appendix E.

A well-controlled CO_2 supply is critical for reliable and competitive electrocatalytic CO_2 conversion routes, as impurities can cause catalyst damage, and CO_2 purification adds extra cost [106]. CO_2 from biogas upgrading (depending on impurities, according to laboratory results [107,108]) or bioethanol production [109–111] were thus considered as relevant options as they are well investigated.

To analyze the effect of an additional incentive to utilize biogenic CO_2, we applied a remuneration mechanism based on CO_2 prices in the European emission trading system (ETS) and the GHG footprint of substituted fossil-based (by)products. GWPs were modeled with GaBi 10.5 [112] (Appendix G).

3.6.4.1. Capital expenditures (CAPEX). CAPEX include the direct costs of equipment purchases, reinvestments for expected replacements during the observation period, and indirect costs.

3.6.4.1.1. Electrocatalytic reaction unit costs. An electrocatalytic reaction unit (ERU) was the main equipment used in the process. Owing to the novelty of this technology and its accordingly low TRL, the expected CAPEX for installation in an industrial environment at an appropriate scale cannot be derived from lab-scale experiments. Thus, for the 2030/ 2040 scenario, significant technological learning and scaling effects were expected.

Owing to the technological similarities of the electrochemical cell used in the ERU with the PEM technology as a common representative for water electrolysis, recent PEM cost development projections, as calculated by Böhm et al. [55] were used. The modularized system costs were calculated for system capacities relevant in the investigated

scenarios, i.e., 11.7 MW (2030) and 5.3 MW (2040), see Table 7.

To consider the impact of the different reaction and conversion efficiencies between the two electrochemical processes on the scaling of equipment costs, the costs of the cell-stack module were converted on an area-related basis for comparison. Other modules listed in Table 7 were presumed to be comparable. The right part of Table 7 summarizes the specific ERU system costs. Compared to the PEM cell, the slightly lower specific cost in 2040 are a result of the effect of technological learning exceeding the effect of downscaling (from 10 to 5 MW). The expected decrease in the power density of the ERU cell prevents an even more significant effect of the learning curve (relating to the electric system capacity).

3.6.4.1.2. Other major equipment. The EEU for C_2H_4 product stream purification and the subsequent EOU for EO synthesis and CH_4 separation were also major components. Their equipment costs are listed in Table 8.

Jouny et al. [73] investigated a concept similar to that of EEU for product separation from different CO_2 electrolysis processes using PSA. Moreover, comparable technologies were considered in a more recent techno-economic study for biogas upgrading [113], which was used as a reference for the estimation of the EEU CAPEX. The CAPEX evaluation of the industry-scale EOU was based on the C_2H_4 epoxidation section described and analyzed by Ghanta et al. [21].

To estimate CAPEX adequate to the evaluated scenarios, the EEU and EOU equipment cost were downscaled using common scaling methods, see Eq. (8) (cf. Peters et al. [98]).

$$C_b = C_a \left(\frac{S_b}{S_a}\right)^f \tag{8}$$

where.

C_a = absolute cost for the reference scale S_a.
C_b = absolute cost at target scale S_b.
f = scaling factor.

3.6.4.1.3. Replacement cost. For some components replacement costs apply as their lifetime is limited compared to the observation period. We considered replacements for the ERU catalyst, which

Table 7

Modularized PEM water electrolysis costs and power specifications for appropriate plant sizes, and specific CAPEX estimates for the ERU accounting for scaling and learning curve impacts based on [55].

Year	Scale	PEM reference cell Module	Costs	Current density	Cell voltage	ERU System costs		Current density	Cell voltage
	[MW]		[€/kW]	[A/cm^2]	[V]	[€/kW]	[Mio. €]	[A/cm^2]	[V]
2030	10	**Overall system**	542.6	2.5	1.6	782	9.12 (11.7 MW)	0.5	4.67
		Cell stack	336						
		Power electronics	122.2						
		Balance of plant	84.3						
2040	5	**Overall system**	274.7	3.1	1.5	745	3.91 (5.25 MW)	0.5	2.1
		Cell stack	141.7						
		Power electronics	83.5						
		Balance of plant	49.5						

Table 8

Initial equipment costs for EEU and EOU, expected replacement cost of equipment during the observation period and addition factors for indirect costs.

Equipment	Cost [Mio. €]	2030	2040	Reference scale	Scaling factor	Notes
EEU	Investment	3.41	2.23	250 m$^3_{in}$/h	0.70	based on[44,54]
EOU	Investment	1.83	1.83	22.6 t$_{out}$/h	0.55	based on[22,49]
Replacement	Cost (cash values) [Mio. €]	2030	2040	Lifetime [years]		
ERU catalyst	Replacements total	9.897	9.902	7		
	Residual value	-0.53	-0.53			
EEU	Replacements total	2.19	1.43	15		
	Residual value	-1.26	-0.82			
Total replacement cost		**10.30**	**9.98**			
Cost factors indirect investment cost (In addition, % of initial CAPEX)		**2030**	**2040**			
Engineering & Supervision		20%				
Construction		30%				
Contingency		25%				

degrades during long-term operation. A replacement of the electrocatalytic stack was assumed every seven years according to Wenderich et al. [97]. Based on an operation time of 8000 FLH per year, this is consistent with the lifetime of approximately 60,000 h expected for PEM water electrolysis cell stacks [55]. In addition to the ERU catalyst, the EEU was presumed to require replacement after 15 years.

All additional equipment was presumed to have a lifetime equal to the observation period of the general TEA, neglecting corresponding replacement cost. The resulting cost are listed in Table 8.

3.6.4.1.4. Indirect cost. Additional indirect costs for peripherals, construction, and engineering were considered using common addition factors found in literature on chemical engineering [98] (Table 8).

3.6.4.2. Operational expenditures (OPEX). OPEX covers the operational and demand-related costs of the electrochemical plant. The material and resource costs are listed in Table 6.

3.6.4.2.1. Electricity demand. Electric power is the major energy source required for electrochemical processes. In the generic scenario, electricity is supplied from the public grid. Therefore, historical spot market data from EXAA [99] were analyzed to obtain a suitable price for green grid electricity (Appendix F). What could be envisioned in recent years is a continuing trend: prices for volatile renewables are fluctuating, and wind and PV power already provide the lowest marginal costs.

The use of renewable electricity was preferred in all scenarios; thus, the average green spot market price was used,[9] which fluctuated around 36 €/MWh for those years. In the sensitivity analysis, the electricity price was varied from − 80% to + 80% to cover the influence of future electricity price changes.

With the use of public electricity grid infrastructure, taxes and fees must be paid, which differ across countries and remain partially unclear for the integration of PtX processes. In a uniform approach, Austrian regulation as of 2021 was used as a reference for all evaluated scenarios.

For direct supply from RES, the projected LCoE for wind and PV in Europe was used, according to relevant literature [56]. The values are listed in Table 6.

3.6.4.2.2. Other material and resource costs. CO_2 and water are other main feedstocks for the process. In all scenarios, CO_2 was assumed to be supplied by local biomethane plants. CO_2 supply cost ranges from 0 to 90 €/t$_{CO2}$, with a tendency towards single-digit values, depending mainly on the capture technology [48]. Furthermore, if CO_2 separation is assumed to be part of biomethane production and the associated costs are allocated accordingly, the CO_2 produced can be valued as a free-of-charge waste stream. Therefore, the CO_2 cost was set at 0 €/kg$_{CO2}$ in the generic case but varied in the sensitivity analysis.

Despite the high water throughput, adequate recirculation of excess

---

[9] Note: While EXAA offers designated green electricity at the spot market, there was apparently no trade based on it according to the analyzed data from 2018 to 2020. Prices from the market data are periodically recurring and have not been market-driven up to this point.
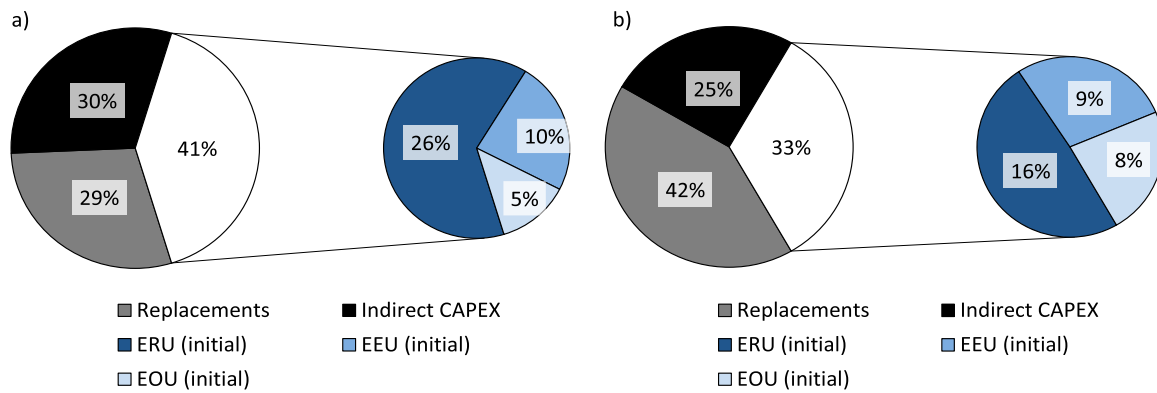
Fig. 7. Individual cost shares of CAPEX in the a) 2030 scenario (total: 35.4 mill. €) and b) 2040 scenario (total: 23.9 mill. €).
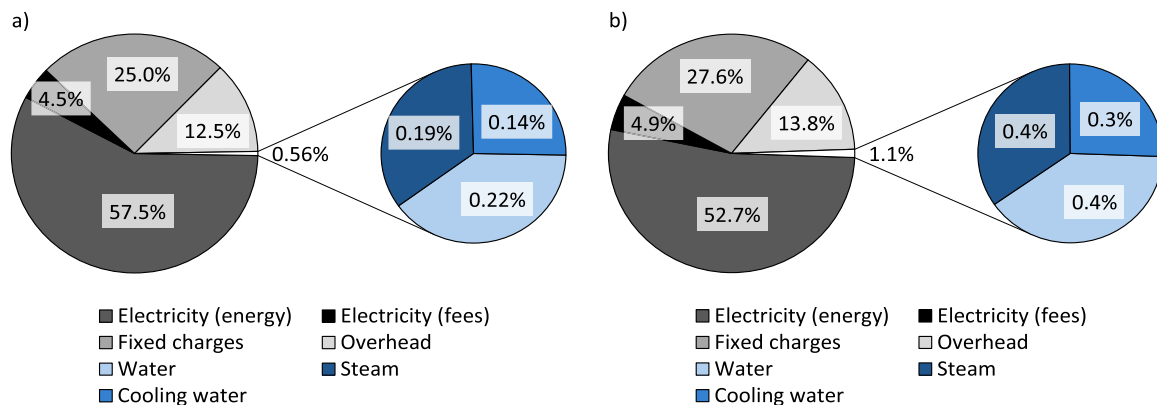

Fig. 8. Individual cost shares of OPEX in the a) 2030 scenario (18.1 k€/day excl. ETS remuneration) and b) 2040 scenario (9.1 k€/day excl. ETS remuneration).

water was assumed. Hence, the demand for freshwater was considered rather small and available at moderate costs [73]. Additionally, steam and cooling water are required for the EOU, and the corresponding costs are considered relative to the epoxidation process investigated by Ghanta et al. [21].

3.6.4.2.3. Fixed charges and overhead. Maintenance and repair must be expected and are therefore considered *ex-ante*. 7% of the initial equipment cost are a reasonable value for annual maintenance and repair costs in process industries [98]. Annual insurance costs are estimated to be approximately 1% of the fixed CAPEX [98].

All these costs directly relate to the operation of the plant. Furthermore, ancillary costs apply to ensure the operation of the plant. These additional costs are summarized as plant overheads, and were considered to be 50% of the fixed OPEX for maintenance, repair, and insurance [98].

4. Results and discussion

The main focus of the following sections is on the generic case with projected implementation in 2030 and 2040, respectively, based on techno-economic performance. The three case studies for Bruck/Leitha, Zerbst, and Isle/Wight are subsequently discussed by a comparison with the generic case.

4.1. Generic case

In the generic case, two plant capacities were evaluated for the corresponding implementation years: 11.67 MW in 2030 and 5.25 MW in 2040.
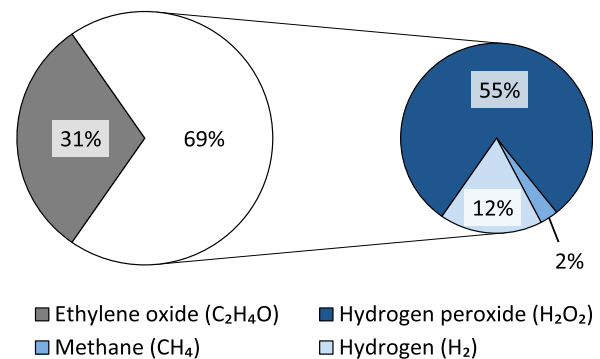

Fig. 9. Revenue shares of products based on the 2030 scenario, in total about 4450 €/day.

4.1.1. Composition of cost shares

To identify potential cost reductions, different cost components were analyzed in detail. Regarding the investment costs for 2030 (Fig. 7/a), the direct CAPEX (i.e., the initial purchase costs for the main equipment) accounts for approximately 41%. Most of these costs are allocated to the ERU (about 63%), whereas the remaining shares are allocated to the direct costs of the EEU and EOU in a ratio of approximately 2:1. Thus, approximately 59% of the total CAPEX is represented by indirect costs, such as engineering and construction costs, as well as expected equipment replacements. For the 2040 scenario, these cost shares are changed (Fig. 7/b). As a result of technological learning effects, the proportion of ERU in the overall CAPEX was reduced to approximately 16%. Moreover, the scaling effects reduced EEU's share of direct investment by approximately one-third. In parallel, the absolute cost of replacements
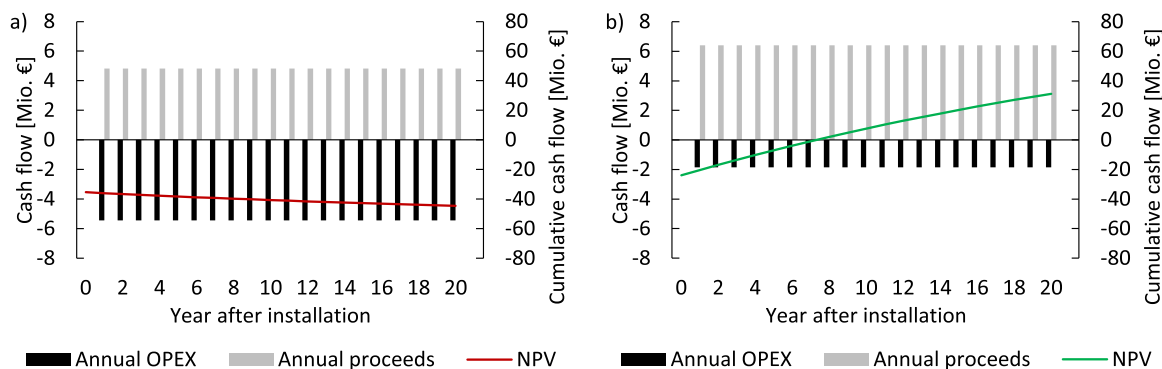
Fig. 10. Development of the net present value (NPV) in the generic scenario for a) 2030 and b) 2040.

decreased insignificantly, leading to an increased cost share of > 40%. Overall, the expected CAPEX for the generic scenarios was estimated to be about 35.4 mill. € for 2030 and 23.9 mill. € for 2040.

For a given plant capacity of 11.67 MW (2030), a total OPEX of 18.1 k€/day was calculated, excluding potential savings due to ETS remunerations. As shown in Fig. 8/a), the largest share of OPEX is represented by the cost of electricity supply (>57%). Due to the less-than-a-half electrical power (5.25 MW) in the 2040 scenario, OPEX were reduced to about 9.1 k€/day, see Fig. 8/b). Considering ETS remuneration as part of the OPEX, the cost reduction would be even more significant because of the expected increase in CO_2 certificate costs.

However, the OPEX cost distribution did not change significantly from 2030 to 2040, regardless of the reduction in electricity supply cost. This is due to the reduction of CAPEX-related fixed charges (operation, maintenance, insurance) and overhead being proportional to the reduction of electricity supply. As the production capacity remains the same for 2030 and 2040, the absolute cost of feedstock and raw materials does not change between scenarios. Thus, the rather low weight of total OPEX on the product generation cost increased slightly from 2030 to 2040.

4.1.2. Product sale revenues

In addition to all cost, revenues from the sale of EO as the target product and individual byproducts, including H_2, CH_4 and H_2O_2, are ultimately relevant to the economic feasibility of the process concept. The assumed sales prices for these renewable chemicals (approximately 4450 €/day and 8900 €/day for 2030 and 2040, respectively) can be achieved by producing and selling EO as the main product. However, assuming that H_2O_2 can be effectively separated and valorized, EO can only account for approximately 31% and 46% of the total revenue in 2030 and 2040, respectively, with 42–55% of the revenue associated with H_2O_2 sales..

In terms of other by-products, particularly H_2 and CH_4, the proposed process must compete with other renewable production methods for these products, such as H_2O electrolysis and methanation, whereby their effective values depend on these concurrent technologies (cf. [55]).

4.1.3. Economic feasibility (NPV and PBT)

For the 2030 scenario, the absolute annual profit is negative (Fig. 10/a), despite considering all potential byproduct sales and savings from the ETS remuneration. Hence, the overall negative annual cash flow would further reduce the NPV, starting from a negative value of − 35.4 mill. € owing to fixed CAPEX (all investments, including replacements
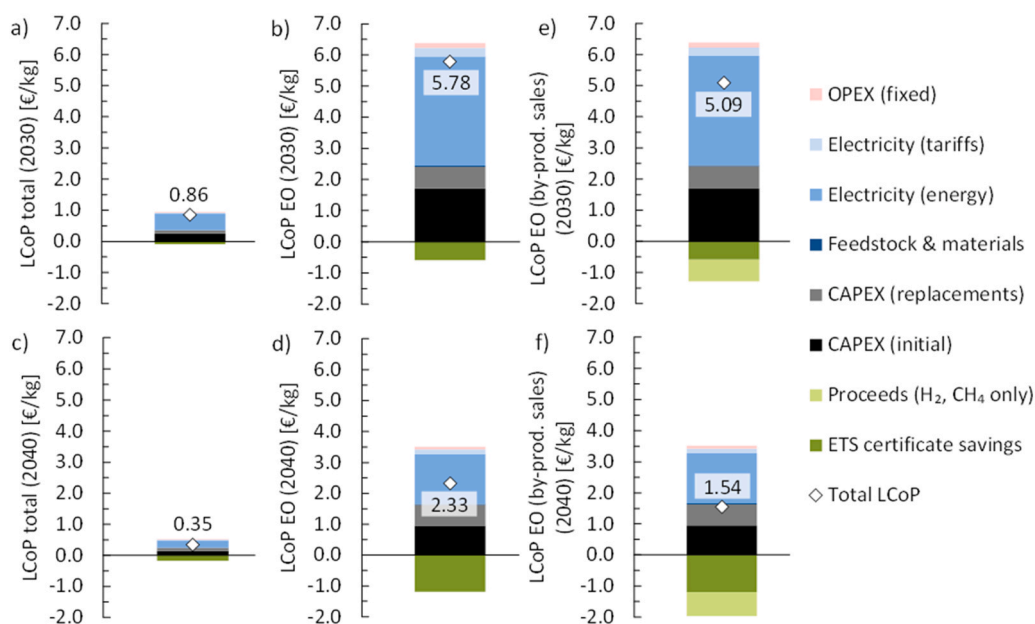

Fig. 11. LCoP composition for the generic scenario: in 2030 related to a) total products and b) EO only without byproduct sales. In 2040 related to c) total products and d) EO only without byproduct sales. Furthermore, the LCoP composition under consideration of byproduct sales (without H_2O_2) for e) 2030 and f) 2040.

discounted to the initial year). Consequently, the calculated PBT would be negative, indicating that the plant is not profitable regardless of the chosen deprecation period.

In the 2040 scenario (Fig. 10/b), the increased revenue due to higher chemical prices would exceed the simultaneously reduced OPEX. Therefore, the NPV increases over the set depreciation period. In addition, a less negative initial value of approx. − 23.9 mill. € (reduced CAPEX), the NPV reaches a positive value in year 5. A corresponding result of 3.3 years was obtained from the static PBT calculation.

These economic results clearly show that CAPEX plays a significant role; however, OPEX must be reduced for the competitive operation of the process. The main lever in this regard is the energy efficiency of the plant, with a special focus on the ERU. Hence, reducing energy costs and investment efforts may result in a process that is economically viable within an acceptable planning interval.

4.1.4. Product generation cost (LCoP)

To evaluate the competitiveness of fossil-based EO production and set appropriate sales prices for renewable products, LCoP is a valuable indicator. Since the process generates significant amounts of valuable byproducts, the LCoP was calculated for both the total product mass including byproducts (H_2, CH_4, H_2O_2) and the mass of EO as the main product alone.

As shown in Fig. 11 a) and b), the average production cost of all chemicals produced in the electrochemical process was calculated to be around 0.86 €/kg$_{product}$ by 2030, which is within the range of the selling prices of the different products considered (Table 6) and in the range of comparable electrochemical processes [28,114]. However, assuming that byproducts cannot be economically exploited and that EO is the only valuable product, the associated LCoP multiplies to about 5.78 €/kg$_{EO}$. Accordingly, the selling prices of such products must be higher than those of fossil-based competitive products.

For the 2040 scenario, the reduced CAPEX and electricity demand will significantly decrease the LCoP, as shown in Fig. 11 c) and d). At ca. 0.35 €/kg$_{product}$, the average cost for all products would be lower than the available prices of fossil-based EO, C_2H_4, and H_2O_2. For the main product alone, an LCoP of 2.33 €/kg$_{EO}$ could be achieved. However, these calculations considered significant ETS remuneration at 100 €/t$_{CO2}$. Without these, the LCoP would increase by 0.18 €/kg$_{product}$ and 1.19 €/kg$_{EO}$ respectively.

If the sale of byproducts in the EO production process is considered for the revenue, the EO-related LCoP decreases further. The effective LCoP for EO, including revenues from H_2 and CH_4, is shown in Fig. 11 e) and f). Owing to the uncertainty of the feasibility of separating excess H_2O_2, the revenues for this byproduct were neglected in these results. Thus, the LCoP amounts to approximately 1.54 €/kg$_{EO}$ in the 2040 scenario, which is competitive with the selling prices of fossil-based products (see Section 3.2).

4.2. Case study comparison

To evaluate the location-based case studies, the same system

capacities as for the generic scenarios were used for comparability. Based on the electric power requirements, the achievable FLH based on the RES potentials at the three locations were calculated on an hourly basis considering the actual usage capacity. The electricity supply costs were weighted according to the LCoE presumed for the individual type of power generation in 2030 and 2040 ([56], see Table 6).

Accordingly, the CO_2 demand must be met by local biogas production, which was found to be feasible: the Isle of Wight and Zerbst biomethane plants could provide 6.7–9.4 times and 2.8–3.5 times the required CO_2, respectively, and thus have the potential for capacity expansion. Therefore, the CO_2 supply is not a bottleneck in these scenarios. Same applies to the generic case, which was based on the Bruck/Leitha conditions.

In the cases of Bruck/Leitha and Zerbst, electricity was (partly) obtained from local wind farms. We found that the annual energy production would be high enough to achieve high annual FLH of > 5500 h/a in 2030 and > 7000 h/a in 2040 (Table 9). This is in the same range as in the generic scenarios. However, these figures are based on the assumption that the process allows for dynamic operation and/or that it is equipped with intermediate electricity storage. In the case of Isle/Wight, only PV power is available, which drastically reduces the annual FLH of the chemical plant if no energy storage is available: < 2000 h/a in 2030 and < 3000 h/a in 2040.

The PBT and LCoP were considered for a techno-economic comparison of the case studies. The PBT is always negative in 2030, which was expected based on the generic results. Thus, no profitable operations are expected to be implemented by 2030. By 2040, the Bruck/Leitha and Zerbst cases are expected to be viable in terms of a short PBT of 3.5–4.0 years. In contrast, the Isle/Wight case reaches amortization after 14 years, which is within the presumed depreciation period of 20 years, but much longer than industry standards.

For all cases, the LCoP based on total product mass is higher than for the generic 2030 scenario. This is because of the higher energy costs and lower annual FLH, especially for Isle/Wight. For 2040, Bruck/Leitha would result in a lower LCoP than the generic scenario because of the presumably low LCoE of wind power in 2040. Meanwhile, on the Isle/Wight, despite lower cost of PV, still low FLH in 2040 lead to nearly twice as high LCoP compared to the generic scenario.

In summary, year-round operation (≥8000 h) of the electrochemical plant concept based on locally produced renewable energy was not possible at any of the three sites. This is true even if the electrochemical plant is given priority in the power supply over the grid feed-in, which is contrary to the idea of balancing the grid with PtX technologies. Supplying the plant with peak energy only, for example, based on a specified base feed-in into the grid, would lead to a further reduction in FLH. As a result, the annual production rate of EO would decrease drastically, whereas CAPEX and some OPEX (such as fixed costs) would remain the same. In other words, the overall profitability of the plants decreased significantly. Despite the additional cost, energy storage appears to be an option for increasing the FLH. However, this leads to the conclusion that the operation of the plant to stabilize the electricity grid is questionable, as this role would be at least partially taken over by the energy

Table 9
Comparison of TEA results for three cases depending on available power supply.

Parameter	Unit	2030			2040		
		Bruck/ Leitha	Zerbst	Isle/ Wight	Bruck/ Leitha	Zerbst	Isle/ Wight
Operation							
Potential FLH[a]	h/a	5864	6150	1959	7170	7745	2742
CO_2 demand	t/a	2198	2305	734	2688	2903	1028
Electricity costs(weighted)	€/MWh	55	55	55	45	38	30
Economic results							
PBT	years	-14.3	-14.3	-14.6	4.0	3.5	14.3
LCoP[b]	€/kg$_{product}$	1.29	1.26	2.38	0.44	0.37	0.82

[a] Potential FLH based on the hourly available electricity production in relation to ERU capacity
[b] Related to total product mass (incl. byproducts) without revenues from byproducts; incl. ETS remuneration
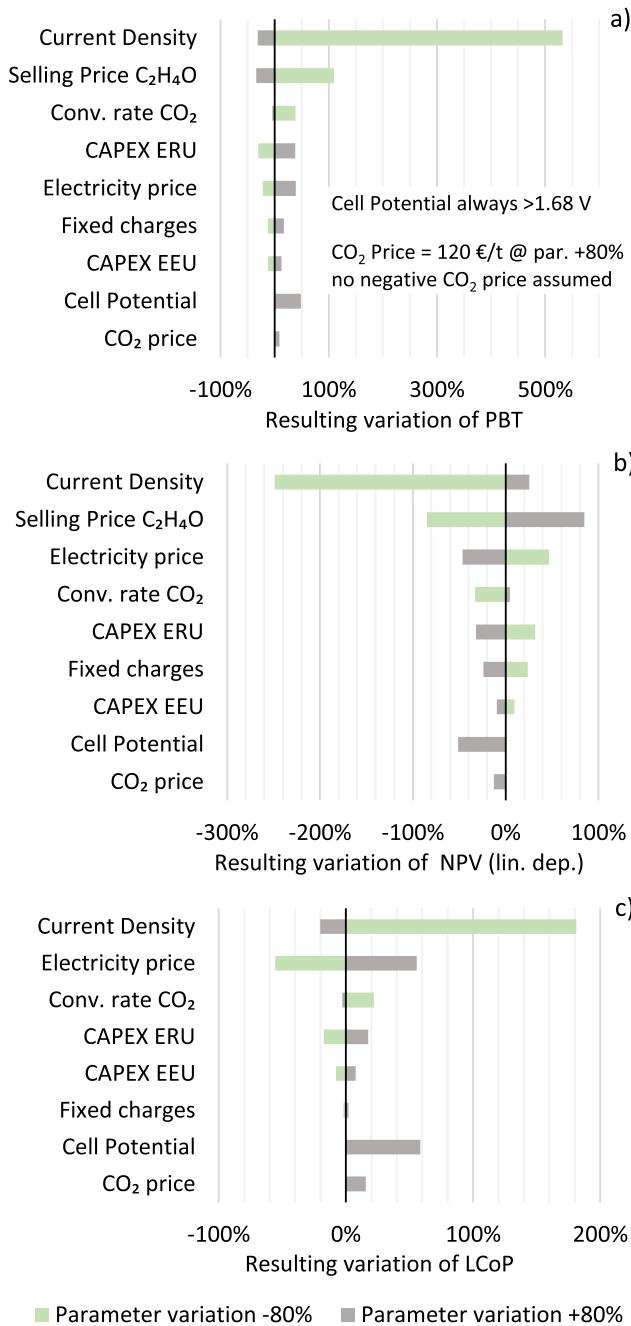
Fig. 12. Relative sensitivity of a) PBT, b) NPV and c) EO-related LCoP to individual parameter variation. Text box in a) applies to a), b), c).
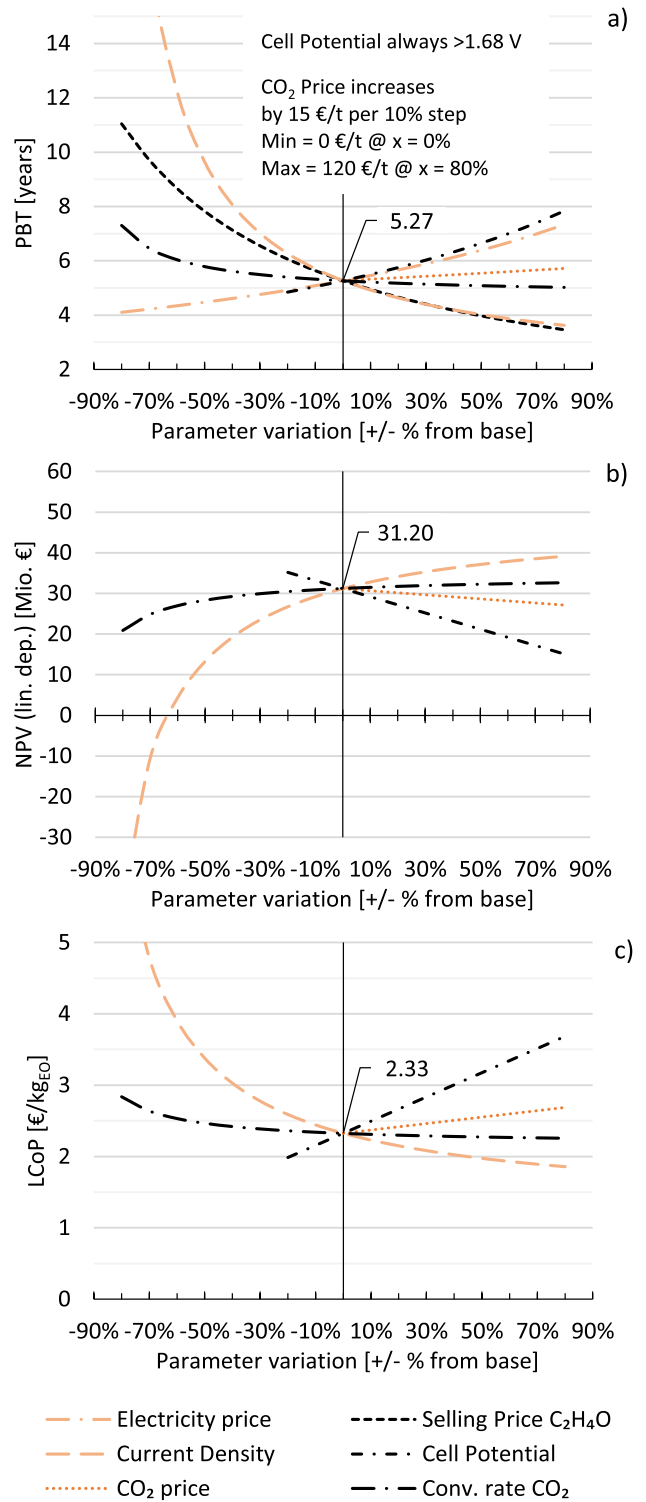

Fig. 13. Absolute sensitivity of a) PBT, b) NPV and c) EO-related LCoP to individual parameter variation with non-linear influence or minimum value variation $> -80\%$. Text box in a) applies to a), b), c).

storage system and possibly lead to reduced plant capacity.

This raises the question of what incentives might lead to the beneficial operation of the electrochemical plant for the electricity grid. For example, reduced electricity prices may reduce the OPEX, although the price difference is unlikely to be recovered by the plant or grid operator. Therefore, public subsidies are essential. However, the achievable selling price of renewable EO and associated green premiums are expected to have a major impact on the overall competitiveness of the process.

4.3. Sensitivity analysis

To assess the impact of the individual calculation parameters on the

evaluated indicators, a sensitivity analysis was performed by varying selected impact factors for the 2040 generic scenario from -80% to $+80\%$. The CO_2 price was varied from 0 to 120 €/t, which covers the range of capture costs (despite DAC) according to [48]. The cell potential reduction was limited to -20%, otherwise the theoretical minimum would be undercut.

Fig. 12 shows the resulting relative change of PBT, NPV and LCoP due to parameter variation. Since some parameters have a non-linear influence (e.g., current density) or had to be varied individually (cell potential, CO_2 price), the absolute change in PBT, NPV and LCoP due to variation of selected parameters is shown in Fig. 13.

4.3.1. Sensitivity of plant profitability

Sensitivity analyses of the PBT (Fig. 12/a, Fig. 13/a) and NPV (Fig. 12/a, Fig. 13/b) showed a strong, non-linear influence of the current density on the electrochemical process: the lower the current density, the larger the cell area and thus the CAPEX increase. A comparable but less significant behavior was observed for the CO_2 conversion rate; a similar effect was expected for the selectivity. However, this could not be tested for the reasons mentioned above (3.6.1). The conversion rate also has an impact on the CAPEX and OPEX associated with the recycling of streams, so it is likely to have a stronger influence than could be detected so far. This should be further investigated in future studies. As expected, the cell potential has a significant impact, as it affects the current density and therefore, the cell area. The most significant impacts of direct CAPEX and OPEX were related to the ERU: the electricity cost was the main cost factor, while the CO_2 cost has a comparatively negligible impact. Finally, the achievable selling price of EO as a renewable chemical is considered to have a major impact on the overall competitiveness of the process.

4.3.2. Sensitivity of production costs

As expected, the LCoP sensitivity analysis (Fig. 12/c, Fig. 13/c) showed a similar behavior to NPV and PBT. As before, the current density had a significant impact, but so had the electricity price and the cell potential, given an equal relative change in parameter. In contrast, the impact of variation in fixed charges (e.g., OPEX for maintenance and insurance) is negligible. CO_2 price and CAPEX are also of secondary importance compared to variable costs. Nevertheless, future studies should also test more detailed variations of component lifetimes and observation period with respect to CAPEX-related impacts and location-related costs (e.g., network tariffs and fees).

4.4. Limitations

This study had several limitations, as described below. Nevertheless, the study provides meaningful results regarding suitable sites and relevant process and economic parameters, that is, it serves as a starting point.

4.4.1. Limited process data

Because the analyzed core technology has a TRL of 3–4, only a simplified equipment list was available. Also, the cathodic product mix is likely to change with further technological advances, depending on multiple factors, from the process design to process operating parameters. For example, promising laboratory results have been obtained in terms of the catalyst and electrode stability in the literature, as well as in the underlying research project (cf. [18,115]): in experiments lasting up to several hours, no signs of degradation were observed. For the TEA however, an optimistic lifetime of 1000 h had to be assumed. Furthermore, the energy efficiency of the process is assumed to increase when the technology reaches TRL 7–9. The latter was partly taken into consideration through the scale-up to the reference years 2030 and 2040.

The first limitation was encountered by adapting known technical and economic conditions of the related technologies, for which cost and efficiency data, as well as learning curves, are available. Furthermore, sensitivity analyses were conducted to demonstrate a realistic range of energy demand and cost development. Moreover, the TEA focused on the main process rather than detailed supply chains or product sales to rule out several uncertain variables that significantly affect the overall result. Product marketing was assumed possible within an acceptable

geographical range. Thus, the case studies were designed with a focus on local resources, that is, short transport routes.

4.4.2. Limitations of GIS-based analysis

The accuracy of spatial potential analysis relies on the quality and completeness of the datasets used. To rule out data errors, data validation and crosschecking were performed via desk research; however, no claim of completeness can be made. As the datasets list production facilities, they are subject to constant change as power plants, biomethane upgrading, and bioethanol plants may be shut down or newly erected over time. Moreover, the capacity and production rates may change over time. Furthermore, information on "production capacity" and "production rate" was not always clearly declared by the data sources. Finally, the data availability per country may vary significantly. For instance, in some countries, more power plants and CO_2 sources may exist than could be identified. In some cases, the locations of the power plants and CO_2 sources were not available via coordinates but could be identified based on their location near cities and/or urban areas to which they were assigned. In particular, urban areas may have a diameter well over 10 km and/or smaller local communities may be assigned to close-by cities in some datasets. Consequently, the locations of various plants were not accurate but sufficient for an approximate analysis of RES and CO_2 potential by a perimeter query. Therefore, the generic scenarios were meant as location-independent reference calculation omitting these limitations.

5. Conclusions

The TEA followed a stepwise approach to identify potential PtX and CCU locations across Europe that offer optimal access to existing CO_2 and renewable electricity sources. Furthermore, a techno-economic assessment for a specific, low TRL CCU process was carried out, including a sensitivity analysis. The process comprised an electrochemical cell with simultaneous C_2H_4 and H_2O_2 production and subsequent EO synthesis.

5.1. Key results

Based on spatial analysis, as biogenic CO_2 sources, 162 biogas plants (equipped with biomethane upgrading) and 13 bioethanol plants, which have wind and/or PV plants > 1 MW in close proximity, were identified for Europe. These locations could serve as a starting point for a fast roll-out of decentralized electrochemical CCU plants, as major supply infrastructure is already available. Based on the assessment of further existing infrastructure, such as chemical parks and ethylene pipelines, three case study locations were derived. In a second step, a TEA was conducted for a generic case and the three locations.

Considering an average production rate of about 1000 t_{EO} per year (analyzed generic case), a theoretical annual EO production volume of 162 kt_{EO} could be reached with the 162 biomethane plants identified. Considering the total biogenic CO_2 amount produced in Europe [48], about 167 Mt_{EO} could be produced. However, only about 1 Mt_{EO} (<3% of the 2030 global market volume [20]) could be produced from the CO_2 already separated from biogas [48], which means with cost and plant infrastructure comparable to this study's assumptions. Also, competing interest of other CCU/PtX operators have to be expected, which further reduces the available CO_2 potential. Similar numbers apply to the byproducts and intermediaries. Furthermore, this will only be

achievable with a significant increase in renewable energy generation (see Fig. 1).

Referring to the ecological impact mentioned in the Introduction, the analyzed route could lead to − 24 to − 79 kt_{CO2eq} considering an implementation at the 162 biomethane plants[10]. Considering a respective reduction of fossil EO production, emissions of about 245 kt_{CO2eq} could be prevented.[10]

Another aspect is that the LCoP of the product mix was approximately 0.86 €/kg (generic scenario), which is within the range of selling prices of different benchmark products considered. Assuming that EO is the only utilizable product, the LCoP increases to about 5.78 €/kg, which exceeds the current EO prices by far.

Sensitivity analysis showed that the process performance factors, specifically with regard to energy efficiency, are among the most determining factors. In parallel, energy cost and CAPEX are equally important in terms of economic feasibility. An extended plant lifetime would be beneficial for reducing the impact of CAPEX.

In other words, the product selling price of EO must be rather high, as the current market price of EO is not sufficient to cover the production cost in the 2030 scenario. For the 2040 scenario with optimized plant conditions and ETS remuneration, a positive NPV may be reached, even with current market prices. Until such optimizations are reached, green premium prices may be an option for early market entry, if customers are willing to pay.

It was shown that high FLH is crucial for profitability. This is contrary to the idea of flattening the grid feed-in of volatile RES using PtX technologies. Energy storage systems can increase the FLH but contradict the initial concept as energy storage could be applied directly to flatten the feed-in. Therefore, the technological concept (sector coupling) and the business model need to be further developed.

5.2. Future outlook

This study touched upon various challenges and open research questions along the supply chain of renewable EO, which is exemplary for other electrocatalytically produced CCU products. Thus, further research in various directions is required.

CO_2 and energy sources.

- While the current biogenic CO_2 potential available at moderate effort is low, we assume that the number of "ideal" sites (biogenic CO_2 and local RES) for electrochemical plants will significantly increase within the next few years, due to European efforts for climate change mitigation. Regular tracking and assessment of the change in potential seems reasonable for further R&D activities.
- Accordingly, CO_2 transport options should be considered to assess potential locations and their impacts on plant profitability
- Furthermore, the variation in CO_2 cost based on the source and separation technology in future TEA seems viable.

Alternative CCU routes

- Competing interests – other CCU/PtX activities – must be tracked as well, to identify synergies and conflict potential, also changes in product demand may become visible with progressing transformation of industry with regard to circularity and sustainability.
- In this regard, extending this study by comparable analyses for other (novel) CCU applications and merging the results in an overall

analysis for the future European CCU market is recommended. On a less detailed scale this is already ongoing work on a global scale [116] and for specific countries (for example CaCTUS [117]).

Novel EO process design

- With advances in experimental and modelling research in cell design, more detailed process data will be available, allowing for more rigorous TEA and detailed sensitivity analysis.
- In that sense, a specific focus should be placed on product selectivities, conversion rates, and energy efficiency.

Novel EO process operation

- Inclusion of start-up and shutdown times and minimum operation of plant for a more detailed analysis of energy supply needs
- Variations in energy supply merit order (PtX plant, energy storage, grid)

Considering the life-cycle costs and measures yet to be implemented (e.g., based on the European circular economy plans), we assume that the proposed technology, if it reaches a higher TRL of 7–9, can witness significant production cost reductions in the future and potentially become competitive with its fossil counterparts. The present TEA and sensitivity analyses identified the predominant triggers towards this development.

CRediT authorship contribution statement

Valerie Rodin: Methodology, Investigation, Formal analysis, Writing – original draft, Writing – review & editing, Visualization. **Hans Böhm:** Methodology, Formal analysis, Validation, Writing – review & editing. **Johannes Lindorfer:** Conceptualization, Funding acquisition, Project administration, Supervision, Methodology, Validation, Writing – review & editing. **Christian Paulik:** Supervision.

Declaration of Competing Interest

The authors declare that they have no known competing financial interests or personal relationships that could have appeared to influence the work reported in this paper.

Data availability

Data will be made available on request.

Acknowledgements

Supporting information

Supplementary data associated with this article can be found in the online version at doi:10.1016/j.jcou.2023.102554.

---

[10] Note: These figures are not derived from consequential LCAs, but are estimates based on attributional LCAs that do not take into account the GHG emissions from an alternative EO production route. A detailed assessment of the consequences of displacement effects (net avoided CO_2 or GHG emissions) is the subject of further R&D, as is the environmental impact of improved energy efficiency and product selectivity.

References

[1] Ferdinand K.ähler, Olaf Porc, Michael Carus, RCI Carbon Flows Report: Compilation of supply and demand of fossil and renewable carbon on a global and European level, nova-Institut, 2023. ⟨https://renewable-carbon.eu/publications/product/the-renewable-carbon-initiatives-carbon-flows-report-pdf/⟩ (accessed July 18, 2023).

[2] European Commission, A European Green Deal, European Commission, 2023. ⟨https://ec.europa.eu/info/strategy/priorities-2019–2024/european-green-deal_en⟩ (accessed June 8, 2023).

[3] UNEP, International Sustainable Chemistry Collaborative Centre, adelphi, IFOK, Forecast chemical market value worldwide from 2025 to 2035, by sector (in billion U.S. dollars), Statista, 2018. ⟨https://www.statista.com/statistics/941962/global-chemical-market-value-by-sector/⟩ (accessed July 18, 2023).

[4] American Chemistry Council, Projection of annual production growth in the global chemical industry by region from 2020 to 2025, Statista, 2020. ⟨https://www.statista.com/statistics/407861/forecast-for-annual-growth-in-chemical-industry-worldwide-by-region/⟩ (accessed July 18, 2023).

[5] J. Mertens, C. Breyer, K. Arning, A. Bardow, R. Belmans, A. Dibenedetto, S. Erkman, J. Gripekoven, G. Léonard, S. Nizou, D. Pant, A.S. Reis-Machado, P. Styring, J. Vente, M. Webber, C.J. Sapart, Carbon capture and utilization: More than hiding CO_2 for some time, Joule 7 (2023) 442–449, https://doi.org/10.1016/j.joule.2023.01.005.

[6] CO2 Value Europe, CCU Projects Database, Database CO2 Value Europe, 2023. ⟨https://database.co2value.eu/projects?utf8=%E2%9C%93&search=&regions=&countries=&tecnology_categories=%2C10%2C6%2C4&process_type_captures=&process_type_utilizations=%2C1%2C19%2C2%2C3%2C5%2C20%2C6%2C7%2C8%2C9%2C18%2C10%2C11%2C12%2C13%2C14⟩ (accessed April 10, 2023).

[7] ZEP, CCS/CCU projects, Zep - Zero Emissions Platform, 2023. ⟨https://zeroemissionsplatform.eu/about-ccs-ccu/css-ccu-projects/⟩ (accessed April 10, 2023).

[8] A. Saravanan, P. Senthil kumar, D.-V.N. Vo, S. Jeevanantham, V. Bhuvaneswari, V. Anantha Narayanan, P.R. Yaashikaa, S. Swetha, B. Reshma, A comprehensive review on different approaches for CO_2 utilization and conversion pathways, Chem. Eng. Sci. 236 (2021) 116515, https://doi.org/10.1016/j.ces.2021.116515.

[9] J. Peng, L. Lu, H. Yang, Review on life cycle assessment of energy payback and greenhouse gas emission of solar photovoltaic systems, Renew. Sustain. Energy Rev. 19 (2013) 255–274, https://doi.org/10.1016/j.rser.2012.11.035.

[10] A. Jäger-Waldau, I. Kougias, N. Taylor, C. Thiel, How photovoltaics can contribute to GHG emission reductions of 55% in the EU by 2030, Renew. Sustain. Energy Rev. 126 (2020), 109836, https://doi.org/10.1016/j.rser.2020.109836.

[11] L.C. Dammeier, J.H.C. Bosmans, M.A.J. Huijbregts, Variability in greenhouse gas footprints of the global wind farm fleet, J. Ind. Ecol. 27 (2023) 272–282, https://doi.org/10.1111/jiec.13325.

[12] World Energy Outlook 2022, Paris, 2022. ⟨https://www.iea.org/reports/world-energy-outlook-2022⟩.

[13] Y. Zhang, Y. Wu, L. Li, Z. Liu, A Hybrid Energy Storage System Strategy for Smoothing Photovoltaic Power Fluctuation Based on Improved HHO-VMD, Int. J. Photo 2023 (2023) 1–13, https://doi.org/10.1155/2023/9633843.

[14] C.S. Makola, P.F. Le Roux, J.A. Jordaan, Comparative Analysis of Lithium-Ion and Lead–Acid as Electrical Energy Storage Systems in a Grid-Tied Microgrid Application, Appl. Sci. 13 (2023) 3137, https://doi.org/10.3390/app13053137.

[15] M. Sharma, S. Dhundhara, R. Singh Sran, Impact of hybrid electrical energy storage system on realistic deregulated power system having large-scale renewable generation, Sustain. Energy Technol. Assess. 56 (2023), 103025, https://doi.org/10.1016/j.seta.2023.103025.

[16] L. Khani, M. Mohammadpourfard, Investigation of a New Methanol, Hydrogen, and Electricity Production System Based on Carbon Capture and Utilization, in: Energy Systems Transition, Springer International Publishing, Cham, 2023, pp. 87–129, https://doi.org/10.1007/978-3-031-22186-6_4.

[17] I. Pavić, N. Čović, H. Pandžić, PV–battery-hydrogen plant: Cutting green hydrogen costs through multi-market positioning, Appl. Energy 328 (2022), 120103, https://doi.org/10.1016/j.apenergy.2022.120103.

[18] V. Rodin, L. Zeilerbauer, J. Lindorfer, C. Paulik, D. Finger, Life cycle assessment of a novel electrocatalytic process for the production of bulk chemical ethylene oxide from biogenic CO_2, Front. Sustain. 3 (2022) 799389, https://doi.org/10.3389/frsus.2022.799389.

[19] C. Kirman, A. Li, P. Sheehan, J. Bus, R. Lewis, S. Hays, Ethylene oxide review: characterization of total exposure via endogenous and exogenous pathways and their implications to risk assessment and risk management, J. Toxicol. Environ. Health, Part B 24 (2021) 1–29, https://doi.org/10.1080/10937404.2020.1852988.

[20] AgileIntel Research (ChemIntel360), Market volume of ethylene oxide worldwide from 2015 to 2021, with a forecast for 2022 to 2029 (in million metric tons), Statista, 2023. ⟨https://www.statista.com/statistics/1245260/ethylene-oxide-market-volume-worldwide/⟩ (accessed April 10, 2023).

[21] M. Ghanta, T. Ruddy, D. Fahey, D. Busch, B. Subramaniam, Is the Liquid-Phase H2O2 -Based Ethylene Oxide Process More Economical and Greener Than the Gas-Phase O2 -Based Silver-Catalyzed Process? Ind. Eng. Chem. Res. 52 (2013) 18–29, https://doi.org/10.1021/ie301601y.

[22] Ethylene Oxide Market And Ethylene Glycol Market- Global Industry Analysis, Size and Forecast 2012–2018, (n.d.). ⟨https://www.transparencymarketresearch.com/ethylene-oxide-and-ethylene-glycol-market.html⟩ (accessed July 7, 2021).

[23] AgileIntel Research (ChemIntel360), Ethylene oxide market value worldwide 2015–2030 | Statista, Statista. (2023). ⟨https://www.statista.com/statistics/1244434/global-market-value-ethylene-oxide/⟩ (accessed July 17, 2023).

[24] ChemAnalyst, Ethylene Oxide Price Trend and Forecast, 2023. ⟨https://www.chemanalyst.com/Pricing-data/ethylene-oxide-1102⟩ (accessed April 11, 2023).

[25] ChemAnalyst, Ethylene Price Trend and Forecast, 2023⟩ ⟨https://www.chemanalyst.com/Pricing-data/ethylene-40⟩ (accessed April 23, 2023).

[26] ChemAnalyst, Mono Ethylene Glycol (MEG) Price Trend and Forecast, 2023. ⟨https://secure.livechatinc.com/⟩ (accessed April 23, 2023).

[27] Y. Gao, L. Neal, D. Ding, W. Wu, C. Baroi, A.M. Gaffney, F. Li, Recent advances in intensified ethylene production—a review, ACS Catal. 9 (2019) 8592–8621, https://doi.org/10.1021/acscatal.9b02922.

[28] J. Sisler, S. Khan, A.H. Ip, M.W. Schreiber, S.A. Jaffer, E.R. Bobicki, C.-T. Dinh, E. H. Sargent, Ethylene Electrosynthesis: A Comparative Techno-economic Analysis of Alkaline vs Membrane Electrode Assembly vs CO_2 –CO–C_2H_4 Tandems, ACS Energy Lett. 6 (2021) 997–1002, https://doi.org/10.1021/acsenergylett.0c02633.

[29] D. Meng, M. Zhang, D. Si, M. Mao, Y. Hou, Y. Huang, R. Cao, Highly Selective Tandem Electroreduction of CO_2 to Ethylene over Atomically Isolated Nickel–Nitrogen Site/Copper Nanoparticle Catalysts, Angew. Chem. 133 (2021) 25689–25696, https://doi.org/10.1002/ange.202111136.

[30] F. Li, A. Thevenon, A. Rosas-Hernández, Z. Wang, Y. Li, C.M. Gabardo, A. Ozden, C.T. Dinh, J. Li, Y. Wang, J.P. Edwards, Y. Xu, C. McCallum, L. Tao, Z.-Q. Liang, M. Luo, X. Wang, H. Li, C.P. O'Brien, C.-S. Tan, D.-H. Nam, R. Quintero-Bermudez, T.-T. Zhuang, Y.C. Li, Z. Han, R.D. Britt, D. Sinton, T. Agapie, J. C. Peters, E.H. Sargent, Molecular tuning of CO2-to-ethylene conversion, Nature 577 (2020) 509–513, https://doi.org/10.1038/s41586-019-1782-2.

[31] S.C. Perry, S.M. Gateman, R. Malpass-Evans, N. McKeown, M. Wegener, P. Nazarovs, J. Mauzeroll, L. Wang, C. Ponce de León, Polymers with intrinsic microporosity (PIMs) for targeted CO_2 reduction to ethylene, Chemosphere 248 (2020), 125993, https://doi.org/10.1016/j.chemosphere.2020.125993.

[32] M. Bisztyga-Szklarz, K. Mech, M. Marzec, R. Kalendarev, K. Szaciłowski, In Situ Regeneration of Copper-Coated Gas Diffusion Electrodes for Electroreduction of CO_2 to Ethylene, Materials 14 (2021) 3171, https://doi.org/10.3390/ma14123171.

[33] C. Lucky, T. Wang, M. Schreier, Electrochemical Ethylene Oxide Synthesis from Ethanol, ACS Energy Lett. 7 (2022) 1316–1321, https://doi.org/10.1021/acsenergylett.2c00265.

[34] S. Impeng, T. Roongcharoen, P. Maitarad, H. Wu, C. Chitpakdee, V. Promarak, L. Shi, S. Namuangruk, High selective catalyst for ethylene epoxidation to ethylene oxide: A DFT investigation, Appl. Surf. Sci. 513 (2020), 145799, https://doi.org/10.1016/j.apsusc.2020.145799.

[35] W. Chung, W. Jeong, J. Lee, J. Kim, K. Roh, J.H. Lee, Electrification of CO_2 conversion into chemicals and fuels: Gaps and opportunities in process systems engineering, Comput. Chem. Eng. 170 (2023), 108106, https://doi.org/10.1016/j.compchemeng.2022.108106.

[36] K. Roh, A. Bardow, D. Bongartz, J. Burre, W. Chung, S. Deutz, D. Han, M. Heßelmann, Y. Kohlhaas, A. König, J.S. Lee, R. Meys, S. Völker, M. Wessling, J. H. Lee, A. Mitsos, Early-stage evaluation of emerging CO 2 utilization technologies at low technology readiness levels, Green. Chem. 22 (2020) 3842–3859, https://doi.org/10.1039/C9GC04440J.

[37] P.D. Mobley, J.E. Peters, N. Akunuri, J. Hlebak, V. Gupta, Q. Zheng, S.J. Zhou, M. Lail, Utilization of CO_2 for Ethylene Oxide, Energy Procedia 114 (2017) 7154–7161, https://doi.org/10.1016/j.egypro.2017.03.1878.

[38] S. Balu, A. Hanan, H. Venkatesvaran, S.-W. Chen, T.C.-K. Yang, M. Khalid, Recent Progress in Surface-Defect Engineering Strategies for Electrocatalysts toward Electrochemical CO_2 Reduction: A Review, Catalysts 13 (2023) 393, https://doi.org/10.3390/catal13020393.

[39] Y. Song, W. Chen, W. Wei, Y. Sun, Advances in Clean Fuel Ethanol Production from Electro-, Photo- and Photoelectro-Catalytic CO2 Reduction, Catalysts 10 (2020) 1287, https://doi.org/10.3390/catal10111287.

[40] H. Wang, J. Xue, C. Liu, Z. Chen, C. Li, X. Li, T. Zheng, Q. Jiang, C. Xia, CO_2 electrolysis toward acetate: A review, Curr. Opin. Electrochem. 39 (2023), 101253, https://doi.org/10.1016/j.coelec.2023.101253.

[41] A. Giuliano, E. Catizzone, C. Freda, Process Simulation and Environmental Aspects of Dimethyl Ether Production from Digestate-Derived Syngas, IJERPH 18 (2021) 807, https://doi.org/10.3390/ijerph18020807.

[42] A. Ateka, P. Rodriguez-Vega, J. Ereña, A.T. Aguayo, J. Bilbao, A review on the valorization of CO_2. Focusing on the thermodynamics and catalyst design studies of the direct synthesis of dimethyl ether, Fuel Process. Technol. 233 (2022), 107310, https://doi.org/10.1016/j.fuproc.2022.107310.

[43] L. Kuo, C.-T. Dinh, Toward efficient catalysts for electrochemical CO_2 conversion to C2 products, Curr. Opin. Electrochem. 30 (2021) 100807, https://doi.org/10.1016/j.coelec.2021.100807.

[44] Y. Yang, F. Li, Reactor design for electrochemical CO_2 conversion toward large-scale applications, Curr. Opin. Green. Sustain. Chem. 27 (2021) 100419, https://doi.org/10.1016/j.cogsc.2020.100419.

[45] B. Rego de Vasconcelos, J.-M. Lavoie, Recent Advances in Power-to-X Technology for the Production of Fuels and Chemicals, Front. Chem. 7 (2019) 392, https://doi.org/10.3389/fchem.2019.00392.

[46] J. Lindorfer, V. Rodin, H. Böhm, K. Fazeni-Fraisl, D7.3: Qualitative evaluation report of socio-economic aspects concerning a roll-out of the specific developed electrocatalytic „simultaneous-factories" and a renewable ethylene oxide market in Europe, Energieinstitut an der JKU Linz, Linz, 2021. ⟨https://co2exide-eu.e-p-c.de/wp-content/uploads/2021/10/CO2EXIDE_D7.3.pdf⟩.

[47] CO2EXIDE, CO2EXIDE – CO2-based electrosynthesis of ethylene oxide, CO2EXIDE – CO2-Based Electrosynthesis of Ethylene Oxide. (2022). ⟨http://co2exide.eu/⟩ (accessed August 4, 2022).

[48] V. Rodin, J. Lindorfer, H. Böhm, L. Vieira, Assessing the potential of carbon dioxide valorisation in Europe with focus on biogenic CO_2, J. CO_2 Util. 41 (2020), 101219, https://doi.org/10.1016/j.jcou.2020.101219.

[49] QGIS, Welcome to the QGIS project!, QGIS A Free and Open Source Geographic Information System, 2023. ⟨https://qgis.org/en/site/⟩ (accessed January 13, 2023).

[50] ePURE, eURE Activity Report 2016–2017, Brussels, 2017. ⟨https://epure.org/media/1559/170531-epure-activity-report-2016–2017.pdf⟩.

[51] European Biogas Association (EBA), Gas Infrastructure Europe (gie), European Biomethane Map 2018: Infrastructure for Biomethane Production, (2018). ⟨http://european-biogas.eu/wp-content/uploads/2018/01/2018.01.09.GIE_BIO_2018_A0_1189x841_FULL_415_clean_final.pdf⟩.

[52] European Biogas Association (EBA), Gas Infrastructure Europe (GIE), European Biomethane Map 2020: Infrastructure for Biomethane Production, (2020). ⟨https://www.europeanbiogas.eu/eba-gie-biomethane-map/⟩.

[53] Enerdata intelligence + consulting, Power Plant Tracker, 2021. ⟨https://www.enerdata.net/research/power-plant-database.html⟩.

[54] The Wind Power, About - The Wind Power - Wind Energy Market Intelligence, 2023. ⟨https://www.thewindpower.net/about_en.php⟩ (accessed January 13, 2023).

[55] H. Böhm, A. Zauner, D.C. Rosenfeld, R. Tichler, Projecting cost development for future large-scale power-to-gas implementations by scaling effects, Appl. Energy 264 (2020), 114780, https://doi.org/10.1016/j.apenergy.2020.114780.

[56] Nuclear Energy Agency (NEA), International Energy Agency (IEA), Projected Costs of Generating Electricity 2020, 2020. https://doi.org/10.1787/a6002f3b-en.

[57] Verein Deutscher Ingenieure e.V., VDI 2067 Blatt 1 - Wirtschaftlichkeit gebäudetechnischer Anlagen: Grundlagen und Kostenberechnung, 2012.

[58] H. Böhm, S. Goers, A. Zauner, Estimating future costs of power-to-gas – a component-based approach for technological learning, Int. J. Hydrog. Energy 44 (2019) 30789–30805, https://doi.org/10.1016/j.ijhydene.2019.09.230.

[59] S. Mavrikis, S.C. Perry, P.K. Leung, L. Wang, C. Ponce de León, Recent Advances in Electrochemical Water Oxidation to Produce Hydrogen Peroxide: A Mechanistic Perspective, ACS Sustain. Chem. Eng. 9 (2021) 76–91, https://doi.org/10.1021/acssuschemeng.0c07263.

[60] D. Pangotra, L.-I. Csepei, A. Roth, C. Ponce de León, V. Sieber, L. Vieira, Anodic production of hydrogen peroxide using commercial carbon materials, Appl. Catal. B: Environ. 303 (2022), 120848, https://doi.org/10.1016/j.apcatb.2021.120848.

[61] S.C. Perry, P. Leung, L. Wang, C. Ponce de León, Developments on carbon dioxide reduction: Their promise, achievements, and challenges, Curr. Opin. Electrochem. 20 (2020) 88–98, https://doi.org/10.1016/j.coelec.2020.04.014.

[62] P. Zakkour, G. Cook, CCS Roadmap for Industry: High-purity CO2 sources Sectoral Assessment – Final Report, Unpublished, 2010. http://dx.doi.org/10.13140/RG.2.1.3717.8722 (accessed July 8, 2021).

[63] F. Ausfelder, A.M. Bazzanella, A. Möller, R. Geres, A. Kohn, S. Lenz, Roadmap Chemie 2050 Auf dem Weg zu einer treibhausgasneutralen chemischen Industrie in Deutschland, 2019. ⟨https://www.researchgate.net/publication/336496114_Roadmap_Chemie_2050_Auf_dem_Weg_zu_einer_treibhausgasneutralen_chemischen_Industrie_in_Deutschland⟩.

[64] PlasticsEurope AISBL, Eco-profiles and Environmental Product Declarations of the European Plastics Manufacturers: Ethylene, Propylene, Butadiene, Pyrolysis Gasoline, Ethylene Oxide (EO), Ethylene Glycols (MEG, DEG, TEG), PlasticsEurope AISBL, Brussels, Belgium, 2012. ⟨https://www.plasticseurope.org/en/resources/eco-profiles⟩.

[65] M. Ghanta, Development of an Economically Viable H2O2-based, Liq. -Phase Ethyl. Oxide Technol.: React. Eng. Catal. Dev. Stud., Diss., Univ. Kans. (2012). ⟨http://hdl.handle.net/1808/11473⟩ (accessed February 18, 2021).

[66] Ecofys, Fraunhofer Institute for Systems and Innovation Research, Öko-Institut e. V, Methodology for the free allocation of emission allowances in the EU ETS post 2012 Sector report for the chemical industry, 2009. ⟨https://ec.europa.eu/clima/sites/clima/files/ets/allowances/docs/bm_study-lime.pdf⟩.

[67] P.P. van Uytvanck, B. Hallmark, G. Haire, P.J. Marshall, J.S. Dennis, Impact of Biomass on Industry: Using Ethylene Derived from Bioethanol within the Polyester Value Chain, ACS Sustain. Chem. Eng. 2 (2014) 1098–1105, https://doi.org/10.1021/sc5000804.

[68] J. Koornneef, P. van Breevoort, C. Hendriks, M. Hoogwijk, K. Koop, M. Koper, IEAGHG, Potential for Biomass and Carbon Dioxide Capture and Storage, IEAGHG, Cheltenham, UK, 2011. ⟨https://ieaghg.org/docs/General_Docs/Reports/2013–11.pdf⟩.

[69] T. Galimova, M. Ram, D. Bogdanov, M. Fasihi, S. Khalili, A. Gulagi, H. Karjunen, T.N.O. Mensah, C. Breyer, Global demand analysis for carbon dioxide as raw material from key industrial sources and direct air capture to produce renewable electricity-based fuels and chemicals, J. Clean. Prod. 373 (2022), 133920, https://doi.org/10.1016/j.jclepro.2022.133920.

[70] M. Fasihi, O. Efimova, C. Breyer, Techno-economic assessment of CO2 direct air capture plants, J. Clean. Prod. 224 (2019) 957–980, https://doi.org/10.1016/j.jclepro.2019.03.086.

[71] M.H. Barecka, J.W. Ager, A.A. Lapkin, Economically viable CO_2 electroreduction embedded within ethylene oxide manufacturing, 10.1039.D0EE03310C, Energy Environ. Sci. (2021), https://doi.org/10.1039/D0EE03310C.

[72] K.A. Adegoke, S.O. Giwa, O.R. Adegoke, N.W. Maxakato, Systematic mapping on the evaluation of electrochemical CO2 conversion to fuels/chemicals/value-added

[73] M. Jouny, W. Luc, F. Jiao, General Techno-Economic Analysis of CO $_2$ Electrolysis Systems, Ind. Eng. Chem. Res. 57 (2018) 2165–2177, https://doi.org/10.1021/acs.iecr.7b03514.

[74] Guidelines for the distribution of Ethylene Oxide (Fourth Revision), Ethylene Oxide and Derivatives CEFIC Sector Group, 2013. ⟨https://www.petrochemistry.eu/wp-content/uploads/2018/01/Guidelines_EO_2013_UK_v6-final.pdf⟩ (accessed April 23, 2023).

[75] Tom Baker, Overcoming ethylene oxide transport challenges, Chemical Watch by Enhesa. (2016). ⟨https://chemicalwatch.com/45724/overcoming-ethylene-oxide-transport-challenges⟩ (accessed April 23, 2023).

[76] Toxicological Profile for Ethylene Oxide, U.S. Department of Health and Human Services, Agency for Toxic Substances and Disease Registry (ATSDR), 2022. ⟨https://www.atsdr.cdc.gov/toxprofiles/tp137.pdf⟩ (accessed April 23, 2023).

[77] P. (Ineos) Skelley, The Trans European Olefins Pipelines Network Project – Benefits to the European Industry, 2008. ⟨https://ec.europa.eu/DocsRoom/documents/11993/attachments/1/translations/en/renditions/native⟩.

[78] ARG, European ethylene pipeline network, ARG. (2016). ⟨https://argkg.com/european-ethylene-pipeline-network/⟩ (accessed July 6, 2021).

[79] UKOPA, UK Ethylene System, (2009). ⟨https://www.ukopa.co.uk/pdfs/UKOPA-09–0016.pdf⟩ (accessed April 11, 2023).

[80] GBST, Interactive Simulation of Pipeline Network - GB Simulation Technology, GB Simulation Technology, 2022. https://gbsimtech.com/?page_id=158 (accessed April 11, 2023).

[81] SABIC, SABIC UK Cross Ctry. Pipelines, SABIC - Chem. That Matters (2023). ⟨https://www.sabic.com/en/about/ehss/sabic-uk-pipelines⟩ (accessed April 11, 2023).

[82] Dep. of Chemistry, University of York, The chemical industry, The Essential Chemical Industry - Online. (2016). ⟨https://www.essentialchemicalindustry.org/index.php/the-chemical-industry/the-chemical-industry⟩ (accessed April 11, 2023).

[83] Petrochemicals Europe, Maps, Refineries and Crackers, Petrochemicals Europe, 2019. ⟨https://www.petrochemistry.eu/about-petrochemistry/petrochemicals-facts-and-figures/maps-refineries-and-crackers/⟩ (accessed July 6, 2021).

[84] S. Pfenninger, I. Staffell, Renewables.ninja: Online RES simulation tool, 2016. ⟨https://www.renewables.ninja/⟩ (accessed February 18, 2021).

[85] Verbund Ag, Windpark Bruck-Göttlesbrunn, 2021. ⟨https://www.verbund.com/de-at/ueber-verbund/kraftwerke/unsere-kraftwerke/windpark-bruck-goettlesbrunn⟩.

[86] VERBUND AG, Windpark Bruck an der Leitha, 2021. ⟨https://www.verbund.com/de-at/ueber-verbund/kraftwerke/unsere-kraftwerke/windpark-bruck-an-der-leitha⟩.

[87] OMV, Raffinerie Schwechat, 2023. ⟨https://www.omv.at/de-at/ueber-uns/raffinerie-schwechat⟩ (accessed April 23, 2023).

[88] European Commission, Joint Research Centre Energy Efficiency and Renewables Unit, JRC Photovoltaic Geographical Information System (PVGIS), 2016. ⟨https://re.jrc.ec.europa.eu/pvg_tools/en/tools.html⟩.

[89] infraleuna, Leuna Site, (2021). ⟨https://www.infraleuna.de/en/leuna-site/tradition⟩ (accessed April 23, 2023).

[90] Pentair Food & Beverage, Haffmans BV, Farmers On The Isle Of Wight Are Now Energy Producers, (2017). ⟨https://www.consorziobiogas.it/wp-content/uploads/2017/02/CS-BIOGAS-WIGHT-FARM-ENERGY-EN-2616.pdf⟩ (accessed April 11, 2023).

[91] H. Böhm, M. Lehner, T. Kienberger, Techno-Economic Assessment of Thermally Integrated Co-Electrolysis and Methanation for Industrial Closed Carbon Cycles, Front. Sustain. 2 (2021) 726332, https://doi.org/10.3389/frsus.2021.726332.

[92] S. Ananthuraj, S. Pitchaimuthu, S. Noda, A review on recent developments in electrochemical hydrogen peroxide synthesis with a critical assessment of perspectives and strategies, Adv. Colloid Interface Sci. 287 (2021), 102331, https://doi.org/10.1016/j.cis.2020.102331.

[93] E. Magori, Energ. für Modellier. (2021).

[94] J. Na, B. Seo, J. Kim, C.W. Lee, H. Lee, Y.J. Hwang, B.K. Min, D.K. Lee, H.-S. Oh, U. Lee, General technoeconomic analysis for electrochemical coproduction coupling carbon dioxide reduction with organic oxidation, Nat. Commun. 10 (2019), 5193, https://doi.org/10.1038/s41467-019-12744-y.

[95] A. Makaruk, J. Lindorfer, V. Rodin, K. Wiesner-Fleischer, E. Magori, D7.1: Virtual demonstrator simulation documentation of the proposed electrocatalytic, simultaneous-factory", 2021.

[96] E. Jeng, F. Jiao, Investigation of CO $_2$ single-pass conversion in a flow electrolyzer, React. Chem. Eng. 5 (2020) 1768–1775, https://doi.org/10.1039/D0RE00261E.

[97] K. Wenderich, B.A.M. Nieuweweme, G. Mul, B.T. Mei, Selective Electrochemical Oxidation of H$_2$O to H$_2$O$_2$ Using Boron-Doped Diamond: An Experimental and Techno-Economic Evaluation, acssuschemeng.1c01244, ACS Sustain. Chem. Eng. (2021), https://doi.org/10.1021/acssuschemeng.1c01244.

[98] M.S. Peters, K.D. Timmerhaus, R.E. West. Plant Design and Economics for Chemical Engineers, 5th ed.,, McGraw-Hill,, New York, 2003.

[99] Energy Exchange Austria (EXAA), Historical Data EXAA Energy Exchange Austria, 2018. ⟨https://www.exaa.at/en/marketdata/historical-data⟩.

[100] Energy Exchange Austria (EXAA), Historical Data EXAA Energy Exchange Austria, 2019. ⟨https://www.exaa.at/en/marketdata/historical-data⟩.

[101] Energy Exchange Austria (EXAA), Historical Data EXAA Energy Exchange Austria, 2020. ⟨https://www.exaa.at/de/marktdaten/historische-daten⟩.

[102] International Energy Agency, World Energy Outlook 2020, OECD, 2020. https://doi.org/10.1787/557a761b-en.

[103] Statista, Ethylene prices globally 2022, Statista, 2020. ⟨https://www.statista.com/statistics/1170573/price-ethylene-forecast-globally/⟩ (accessed June 29, 2021).

[104] ChemAnalyst, Hydrogen Peroxide Prices, News, Market Analysis, Monitor, 2022. ⟨https://www.chemanalyst.com/Pricing-data/hydrogen-peroxide-1169⟩ (accessed April 11, 2023).

[105] Eurostat, Gas prices for non-household consumers - bi-annual data (from 2007 onwards): nrg_pc_203, 2020. ⟨http://ec.europa.eu/eurostat/product?code=nrg_pc_203⟩.

[106] R.L. da Silva Pinto, A.C. Vieira, A. Scarpetta, F.S. Marques, R.M.M. Jorge, A. Bail, L.M.M. Jorge, M.L. Corazza, L.P. Ramos, An overview on the production of synthetic fuels from biogas, Bioresour. Technol. Rep. 18 (2022), 101104, https://doi.org/10.1016/j.biteb.2022.101104.

[107] F. Réti, G. Kiss, K. Szaciłowski, K. Wiesner-Fleischer, D. Pangotra, S. Mavrikis, D6.6: Final report on operating conditions and influence of (poisoning) contaminations on CO2 reduction and the water oxidation reaction obtained from lab devices, 2021.

[108] AXIOM, D2.2: "Biogas upgrading off-gas stream analysed," 2018.

[109] P. Bains, J. Moorhouse, Biofuels – Analysis Tracking Report 2022, IEA. (2022). ⟨https://www.iea.org/reports/biofuels⟩ (accessed April 11, 2023).

[110] A. Laude, O. Ricci, G. Bureau, J. Royer-Adnot, A. Fabbri, CO2 capture and storage from a bioethanol plant: Carbon and energy footprint and economic assessment, Int. J. Greenh. Gas Control 5 (2011) 1220–1231, https://doi.org/10.1016/j.ijggc.2011.06.004.

[111] Q. Zhang, Nurhayati, C.-L. Cheng, D. Nagarajan, J.-S. Chang, J. Hu, D.-J. Lee, Carbon capture and utilization of fermentation CO_2: Integrated ethanol fermentation and succinic acid production as an efficient platform, Appl. Energy 206 (2017) 364–371, https://doi.org/10.1016/j.apenergy.2017.08.193.

[112] Sphera, Life Cycle Assessment (LCA) Software | Sphera, LCA for Experts (GaBi). (2023). ⟨https://sphera.com/life-cycle-assessment-lca-software/⟩ (accessed July 10, 2023).

[113] M. Ellerstorfer, M. Harasek, Greening the gas"; Task 3.2: Standardisierte Aufbereitung CH4-basierter biogener Gase, Montanuniversität Leoben (VTiU), 2020. ⟨https://www.gruenes-gas.at/assets/Uploads/2-Montanuniversitat-Leoben-2019-Entwicklung-eines-Standard-Konzept-Aufbereitung-Rohbiogas.pdf⟩.

[114] M.G. Kibria, J.P. Edwards, C.M. Gabardo, C. Dinh, A. Seifitokaldani, D. Sinton, E. H. Sargent, Electrochemical CO_2 Reduction into Chemical Feedstocks: From Mechanistic Electrocatalysis Models to System Design, Adv. Mater. 31 (2019), 1807166, https://doi.org/10.1002/adma.201807166.

[115] CO2EXIDE, CO2EXIDE – Journal publications, 2021. ⟨https://co2exide-eu.e-p-c.de/publications/⟩ (accessed April 30, 2023).

[116] V. Sick, G. Stokes, F. Mason, Y.-S. Yu, A. Van Berkel, R. Daliah, O. Gamez, C. Gee, M. Kaushik, Implementing CO2 capture and utilization at scale and speed, Global CO2 Initiative Research Collection, 2022. https://doi.org/10.7302/5825.

[117] CCCA, Energieinstitut an der JKU Linz, Montanuniversität Leoben, denkstatt, CaCTUS – Austria's climate neutrality: An in-depth evaluation of the potential contribution of CCU and CCS for the Austrian long-term climate goals, project-cactus.at., 2023. ⟨https://project-cactus.at/⟩ (accessed July 18, 2023).